Quaternary Science Reviews 263 (2021) 107003

Contents lists available at ScienceDirect

Quaternary Science Reviews

journal homepage: www.elsevier.com/locate/quascirev

LiDAR-based quantitative assessment of drumlin to mega-scale glacial lineation continuums and flow of the paleo Seneca-Cayuga paleo-ice stream

Shane Sookhan [a, *], Nick Eyles [a], Syed Bukhari [a], Roger C. Paulen [b]

[a] Department of Physical and Environmental Sciences, University of Toronto at Scarborough, 1065 Military Trail, Scarborough, Ontario, M1C 1A4, Canada
[b] Geological Survey of Canada, 601 Booth Street, Ottawa, Ontario, K1A 0E8, Canada

ARTICLE INFO

Article history:
Received 4 February 2021
Received in revised form
10 May 2021
Accepted 24 May 2021
Available online 9 June 2021

Handling Editor: C. O'Cofaigh

Keywords:
New York finger lakes
Subglacial bedform continuum
Flow units
Ice stream

ABSTRACT

Shortly after 14,500 ybp during the deglaciation of the Laurentide Ice Sheet in eastern North America, the 80 km wide Seneca-Cayuga paleo ice stream occupied the overdeepened New York State Finger Lake basins. The topography of the former ice stream bed can be evaluated from high-resolution LiDAR DEM data, allowing mapping of almost four thousand subglacially streamlined bedforms such as drumlins and mega-scale glacial lineations using Curvature-based Relief Separation. Qualitative and quantitative techniques were then applied to the statistical analysis of bedform elongation ratio and orientation using Natural Neighbor Interpolation and unsupervised machine learning-based data clustering. Analysis reveals a geomorphic continuum of as many as seven morphotypes of streamlined bedforms from drumlins to mega-scale glacial lineations with intermediate 'channeled drumlins' possibly recording erosion of parent drumlins. Spatial analysis using orientation Grouping Analysis identifies several flow-parallel sets of bedforms reflecting the presence of multiple ice flow units in the ice stream up to 10 km wide that were topographically controlled by glacially-overdeepened basins of lakes Canandaigua, Seneca, and Cayuga (−151, −306, −242 below mean sea level respectively). Longitudinal variation in bedform elongation along as much as 60 km length of flow lines is provisionally interpreted as a proxy for ice flow velocities which ranged from steady state flow (drumlins), intermediate velocities (channeled drumlins) to fast flow (mega-scale glacial lineations). Evolution in bedforms occurred rapidly likely over a time frame of several hundred years. Quantitative data also identifies faster axial flow and slower flow along the margins of each ice flow unit. Fast flow was triggered at the grounding lines of flow units terminating in deep (as much as 600 m) proglacial lakes at the southern end of each overdeepened Finger Lake basin and propagated northwards along each flow unit at different rates reflecting the size and depth of frontal waterbodies. Petrographic data from tills derived from distinctive Paleozoic quartzites outcropping in a narrow west-east belt perpendicular to flow of each ice stream identifies extended longitudinal subglacial advection during fast flow consistent with very rapid bedform evolution.

1. Introduction

There is a wealth of geomorphological and paleoglaciological information inscribed on the now exposed beds of Pleistocene ice sheets in the form of streamlined bedforms such as drumlins and mega-scale glacial lineations (e.g., Ross et al., 2009; Stokes, 2011; Stokes et al., 2016; Ó Cofaigh et al., 2013; Evans et al., 2014; Spagnolo et al., 2014; Ely et al., 2016; Barchyn et al., 2016; Otteson et al., 2016; Eyles et al., 2016, 2018). With the availability of LiDAR-derived topographic mapping and statistical packages, this geomorphic information can now be translated into quantitative and qualitative paleoglaciological data in a greater level of detail than attainable previously (e.g., Spagnolo et al., 2012; Dowling et al., 2015; Yu et al., 2015; Ely et al., 2016; Sookhan et al., 2016, 2018; Putkinen et al., 2017). With this objective in mind, the present paper develops and tests a systematic approach for assessing paleo ice stream dynamics from high resolution geomorphological data. This was achieved by using geospatial analytical techniques and hierarchical and unsupervised machine learning-based data

* Corresponding author.
E-mail address: shane.sookhan@mail.utoronto.ca (S. Sookhan).

https://doi.org/10.1016/j.quascirev.2021.107003

clustering. Curvature-based Relief Separation (CBRS) was used to map bedforms from high-resolution LiDAR-derived Digital Elevation Model (DEM) data to create a large geomorphic database containing the width, length, height, elongation ratio and orientation of almost 4000 subglacial bedforms in upper New York State. Bedform orientation and elongation ratio are analogues for both ice flow direction and velocity respectively (Smalley and Unwin, 1968; Stokes and Clark, 2002) and are qualitatively evaluated here using Natural Neighbor interpolation. This qualitative assessment is then used to inform more advanced hierarchical and unsupervised machine learning clustering algorithms that can quantify those relationships.

The methodology described herein is used to examine the bed of a large ~80 km wide and ~100 km long Late Wisconsin ice stream in the Finger Lakes region of upper New York State that was triggered sometime shortly after 14,500 ybp during regional deglaciation of the Laurentide Ice Sheet (LIS) (Sookhan et al., 2018a). We identify the composite glaciological structure of the former ice stream by recognising several longitudinal ice flow units, and continuums of bedforms on the bed of each one flow unit ranging from drumlins to mega-scale glacial lineations (MSGLs) with several intermediate morphotypes.

1.1. Regional and physical setting

The Finger Lakes of upper New York State are cut into the high standing surface of the Allegheny Plateau which regionally is characterized by a well-developed 'pre-glacial' dendritic drainage system. This drains southwards down the regional dip of underlying Lower Paleozoic sedimentary strata into the Susquehanna River system (Fig. 1). The lakes are as deep as 200 m and occupy narrow steep-sided bedrock basins that now extend southwards as much as 70 km into the plateau. These basins have variably been called 'through valleys' (Tarr, 1894, 1905; Monnett, 1924; Holmes, 1937; Muller, 1965a,b; Muller and Prest, 1985; Muller and Cadwell, 1986; and Cadwell and Muller, 2004), 'intrusive troughs' (Clayton, 1965, 1972, 1972; Coates, 1974) and 'fiord lakes' (Eyles et al., 1991). The largest of these basins (Otisco, Skaneateles, Owasco, Cayuga, Seneca, Keuka, and Canandaigua; Figs. 1 and 2) radiate outward to the south much like the fingers on an opened outstretched hand, extending from a notional 'wrist' just east of the city of Rochester (with the thumb represented by Oneida Lake). The study area lies immediately south of the deepest part of Lake Ontario (the Rochester Basin at - 244 m below mean sea level; bmsl; Virden et al., 1999) indicating this area has been a locus for enhanced glacial erosion over numerous glacial cycles. Bathymetric data collected in the course of marine-based high-resolution seismic reflection surveys of the Finger Lakes by Syracuse University and the University of Toronto show that the bedrock floors of Canandaigua, Seneca, and Cayuga lakes are also over-deepened well below mean sea level (−151, −306, −242 m bsl respectively; Mullins and Eyles, 1996 and references therein) and further, that their sediment fills accumulated during a single phase of rapid proglacial lacustrine sedimentation during ice retreat, testifying to the removal of any pre-existing fill by glacial erosion.

The precise origin(s) of the Finger Lake basins is still unclear after more than a century of study (Chamberlin, 1883; Tarr 1894, 1905; Clayton, 1972; Muller et al., 1988; Bloom, 2018). The possible role of LIS ice streams in selective downcutting and excavation was first suggested by White (1985) and Mullins and Hinchey (1989). Subsequently, Mullins et al. (1996) invoked rapid erosion during a single phase of Late Wisconsin ice streaming coincident with

Fig. 1. LiDAR-generated topography of Finger Lakes region of Upper New York State, USA and contiguous parts of Ontario north of Lake Ontario and simplified distribution of Valley Heads Moraine (in black). Inset shows location of study area (Fig. 2).

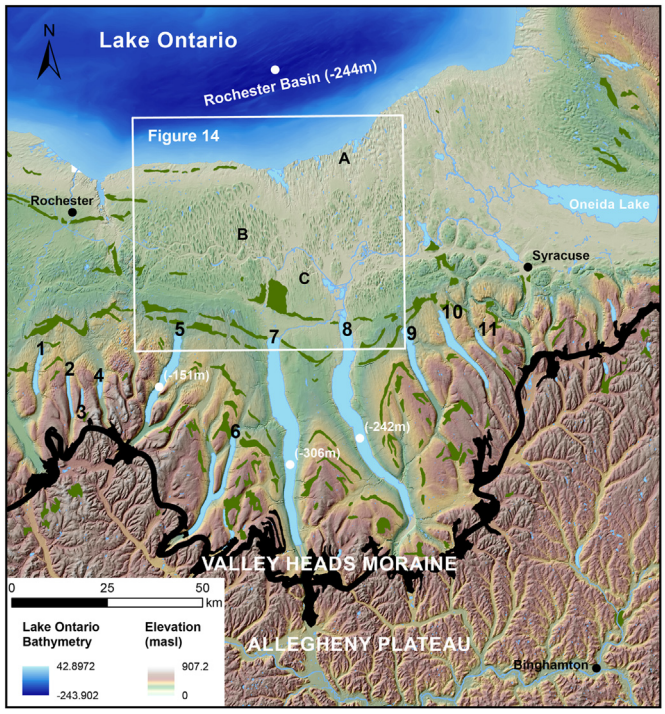

Fig. 2. LiDAR-based Hillshaded DEM map of Finger Lakes study area (Fig. 1). Valley Heads Moraine (in black) was deposited at c. 14.5 ka and marks the southernmost limit of mega-scale glacial lineations recording topographically confined ice streams moving into the Finger Lake basins. End moraines to north (in green) record still-stands during incremental retreat of the LIS margin. Numbers identify individual lake basins 1: Conesus, 2: Hemlock, 3: Canadice, 4: Honeoye, 5: Canandaigua, 6: Keuka, 7: Seneca, 8: Cayuga, 9: Oswaco, 10: Skaneateles, 11: Otisco. Maximum lake depths are shown in in metres below mean sea level. Location of Fig. 13 is shown in inset. Locations of Fig. 3 A-C lettered. (For interpretation of the references to color in this figure legend, the reader is referred to the Web version of this article.)

Heinrich Event 1 (Hemming, 2004; Stanford et al., 2011) but specific geomorphological evidence for the former presence of ice streams was lacking from their model. The paleo ice stream hypothesis of Mullins and Hinchey (1989) was rejected by Ridky and Bindschadler (1990) in favour of long-term erosion under more slowly flowing outlet glaciers based largely on inferred values of basal shear stress. Later work by Hart (1999), Kerr and Eyles (2007) and Briner (2007) recognized 'megaflutings' within the drumlins of Upper New York State and interpreted them as a record of faster flowing ice that Hess and Briner (2009) suggested had been topographically controlled. More recently, in their review study of LIS paleo ice streams Margold et al. (2015a and b, 2018) depicted a single large west-flowing paleo ice stream along the axis of the Ontario Basin but analysis of LiDAR data now reveals numerous additional ice streams in the eastern Great Lake sector of LIS based on mapping of flow units of mega-scale glacial lineations (Sookhan et al., 2018a, b; 2019). These data also reveal a wider range of subglacial bedform morphometries previously imperceivable from previously published datasets (Fig. 3). One large paleo ice stream (the Seneca-Cayuga Ice Stream) flowed south into the Finger Lakes from the overdeepened Ontario Basin to terminate along the complex hummocky ice-contact deposits of the Valley Heads Moraine system (VHM: Fig. 1). This distinctive depositional system is dominated by chaotically-bedded outwash much of its deposited subaqueously, that locally reaches thicknesses of 250 m. Sediments accumulated in deep water along the margins of ice flowing southwards through individual Finger Lake basins (Wellner et al., 1996; Kappel and Miller, 2003; Karig and Miller, 2020). The VHM marks the position of the LIS margin sometime between ~14.8 and 13.6 ka (Ridge et al., 1991, 2012, 2012; Muller and Calkin, 1993; Mullins et al., 1996; Ridge, 2003; Millar, 2004; Franzi et al., 2016; Bloom, 2018).

2. Methods

Sookhan et al. (2018a) provided a broad review of subglacial bedform types in upper New York State and with further field and laboratory investigation, it became apparent that there is significant spatial variation in streamlined bedforms that could be systematically mapped and statistically quantified. Quantitative and qualitative ice flow dynamic data were derived in the present study from high-resolution LiDAR topographic data in four principal

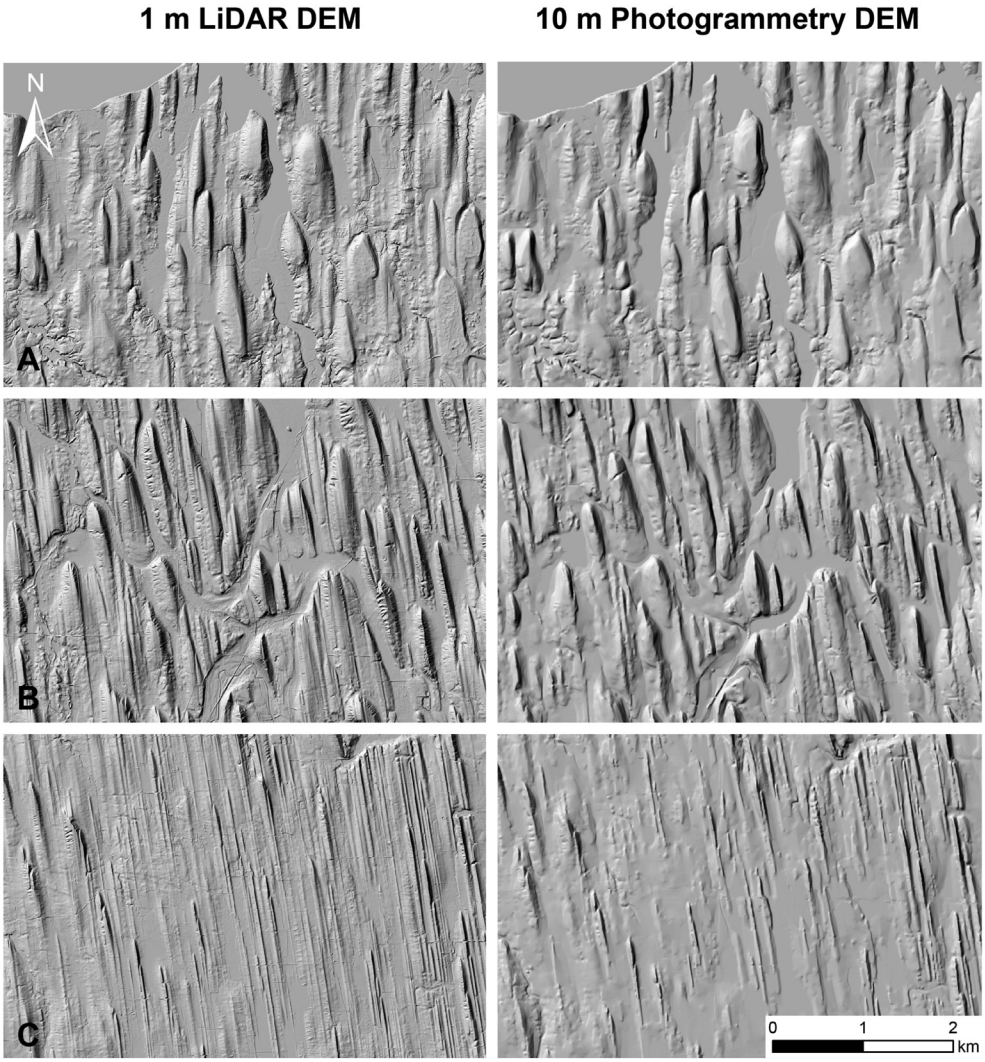

Fig. 3. 1-Meter LiDAR-based DEM data compared with 10-m Photogrammetry DEM data illustrating the importance of newly available high-resolution imagery for mapping the full range of subglacial bedform morphologies needed to derive detailed paleo-glaciological data. Panel 'A' shows area predominately covered by drumlins, 'B' 'channeled' drumlins, and 'C' mega-scale glacial lineations. Note the lack of grooving and low relief lineations visible in the 10-m data.

steps: (1) Data Acquisition and Preparation, (2) Subglacial Bedform Mapping, (3) Data Interpolation, and (4) Data Clustering. The topographic dataset assembled for the present study was prepared from the best available high-resolution digital elevation model (DEM) data for the Finger Lakes Region and used to map subglacial bedforms using the semi-automated Curvature-Based Relief Separation (CBRS) mapping tool. The mapped bedforms were then used to calculate morphometric parameters such as elongation ratio and orientation which have been shown by previous workers to be characteristic of ice flow direction and velocity, respectively. These morphometric parameters were then analysed using Natural Neighbor data interpolation to visualise broadscale patterns in bedform orientation and elongation across the study area and qualitatively identify which parameters were spatially clustered and which were non-spatially clustered. These qualitatively identified relationships were then quantified using the hierarchical algorithm-based Grouping Analysis (GA) tool for clustering spatially constrained morphometric parameters and the unsupervised machine learning-based K-Means clustering for non-spatially constrained parameters. The paleo-glaciological significance of the quantitatively identified data clusters were then explored using summary statistics and by producing maps to analyse their geographical distribution. The above steps represent a new framework for describing ice flow dynamics from high-resolution topographic data and are described in detail in the following subsections and summarized in Fig. 4.

2.1. Data acquisition and preparation

The study was conducted using a large (~170,450 km^2 and >500 Gb) DEM-based map compiled from a variety of high-resolution datasets (collected by the Federal Emergency Management Agency of USA, the United States Department of Agriculture, the United States Geological Survey, and Ontario Natural Resources and Forestry) with raster cell resolutions of less than or equal to 5 m and with most of the data being LiDAR derived (all data sources are summarized in Fig. 4). All datasets were processed with ArcMap v10.7. To create a dataset for mapping and analysis of glacial bedforms, each sub-dataset was resampled to a 5 m cell resolution and then mosaicked into a single uniform and seamless DEM, hereby referred to as the source DEM. The source DEM was projected with the Universal Transverse Mercator (UTM) zones 18 N horizontal coordinate system and the horizontal datum North American Datum 1927 with elevation measured in metres above mean sea level. The source DEM was processed into a hillshade using 4-times vertical exaggeration, a light source azimuth of 315° and an incident angle of 45°. This hillshade was overlain with the source DEM and used for visualization (Fig. 2).

2.2. Subglacial bedform mapping

Drumlins and MSGLs were mapped from the source DEM to reconstruct the ice flow dynamics in the study area using Curvature-based Relief Separation (CBRS). This methodology was specifically developed by Yu et al. (2015) and Sookhan et al. (2016, 2018a) for mapping subglacial landforms from high-resolution DEM imagery and is referred to as a semi-automated method because it does not rely on user input for the initial mapping and only requires subjectivity in the error correction stage. The final output of the CBRS method was an ArcGIS shapefile containing polygons with an associated attribute table containing the calculated morphometric parameters including length, width, elongation ratio (length/width), height and long axis orientation (measured clockwise from north) of each bedform (Fig. 5). The elongation ratio and orientation were used as the input parameters for the subsequent data interpolation and data clustering steps, with the remaining parameters examined in the summary statistics of both analyses.

2.3. Data interpolation

Data interpolation is a powerful tool for drawing widescale interpretations from spatially separated point sources (e.g., Paulen et al., 2006; Ng and Hughes, 2019). Four data interpolation methods were evaluated for the analysis of spatial patterns in elongation ratio and orientation of some 4000 mapped CBRS bedforms using ArcMap v10.7.1. These are Spline, Inverse Distance Weighting (IDW), Kriging, and Natural Neighbor (NN) interpolation. This part of the investigation was completed by converting the CBRS mapped polygons into points to be used as the input sample points for the interpolation algorithms that were each run at a cell size of 10 m. The NN (or Sibson "area-stealing") interpolation method of Sibson (1981) uses Voronoi polygons to find the closest subset of input samples to a query point and then uses these points to create weights based on nearby proportionate unsampled areas to interpolate the value of these areas. Since it only uses sampled points to interpolate, and does not infer trends, it does not produce peaks, pits, or ridges, that were not present in the input samples (Sibson, 1981), making it ideal for qualitative visual analysis of broad patterns in ice flow behaviour.

The NN raster image interpolated for both elongation ratio and orientation were overlain on the hill-shaded DEM data, with the colour intensity in each raster image corresponding to increased elongation and changes in bedform orientation measured clockwise from north respectively. Patterns in the color intensity of both the NN interpolated elongation ratio and orientation rasters were then visually assessed to qualitatively determine both ice flow dynamics and the presence or absence of spatially or non-spatially constrained clustering. Clustering was determined from the NN raster images by looking for repeated patterns of color intensities, with spatially constrained clustering identified by the presence of geographically separated regions of similar color intensity.

2.4. Data clustering

The bedform elongation ratio and orientation datasets were used as the input for either non-spatially or spatially constrained data clustering algorithms depending on the result of the visual assessment of the NN-derived raster images described above. In the context of this study spatial constraint refers to the use of bedform spacing as a clustering parameter. The data clustering effectiveness and the precise number of clusters statistically determined to occur within each dataset was then validated and evaluated, with the summary statistics and geographic distributions of the clusters analysed to assess paleo-glaciological behaviour.

2.4.1. Non-spatially constrained data clustering

This study used an unsupervised machine learning data clustering algorithm called K-Means to cluster parameters that were determined to be non-spatially constrained. The K-Means algorithm takes a dataset (X) with N points as an input and evaluates whether there are K clusters within the dataset, with the output being a set of K cluster centroids where all points within a cluster are closer in distance on an outputted plot to their centroid than they are to any other centroid (Faber, 1994). This is expressed mathematically as follows:

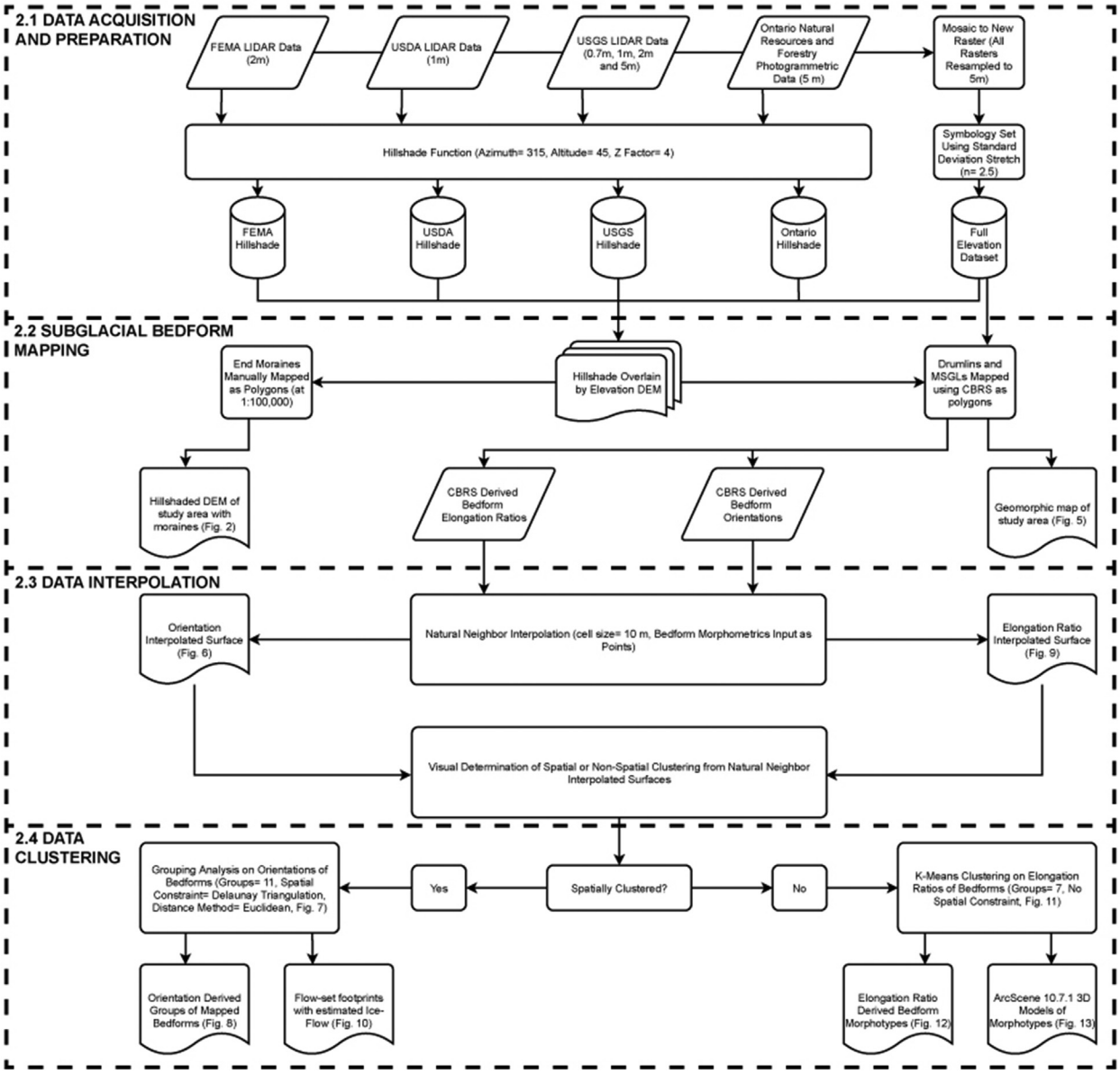

Fig. 4. Flowchart summarizing the methodological steps taken to acquire and analyse LiDAR-based elevation data to identify and map subglacial bedforms in the Finger Lakes region. Headings correspond to Methodology section headings. FEMA - Federal Emergency Management Agency, USDA - United States Department of Agriculture, USGS - United States Geological Survey.

$$Minimize \sum_{k=1}^{K} \sum_{x_n \in C_k} x_n - \mu_k{}^2$$

where C_k is the number of clusters and μ_k is the cluster centroids.

This study used an iterative learning method to solve this called Lloyd's algorithm which uses two operations to (1) update μ_k for C_k whenever there is a closer centroid and (2) given C_k recalculate μ_k as the means of all points belonging to a cluster:

$$C_k = \{x_n : x_n - \mu_k \leq all\, x_n - \mu_n\} \quad (1)$$

$$\mu_k = \frac{1}{C_k} \sum_{x_n \in C_k} x_n \quad (2)$$

This was implemented in Python 3.7 using the *scikit-learn* and *pandas* packages. The geomorphometric data was exported from ArcMap 10.7 as a CSV file and then imported into a *pandas dataframe* in Python to be used as the input for the K-means clustering function in *scikit-learn* with the number of clusters (K) set to 2–15.

2.4.2. Spatially constrained data clustering

Spatially constrained data clustering considers bedform spacing along with the geomorphometric parameter of interest and was accomplished in this study with a hierarchical clustering algorithm using the Grouping Analysis (GA) tool in ArcMap 10.7. This technique organizes a number of features (n) into classes or groups (n_c) based on the statistically similarity of a specified attribute. To group the bedforms the mapped polygons from the CBRS output were used as an input for GA with the Delaunay Triangulation method as the spatial constraint. The parameters used were determined by the qualitative analysis of the NN interpolated images as described above. It is important to note that each parameter (bedform

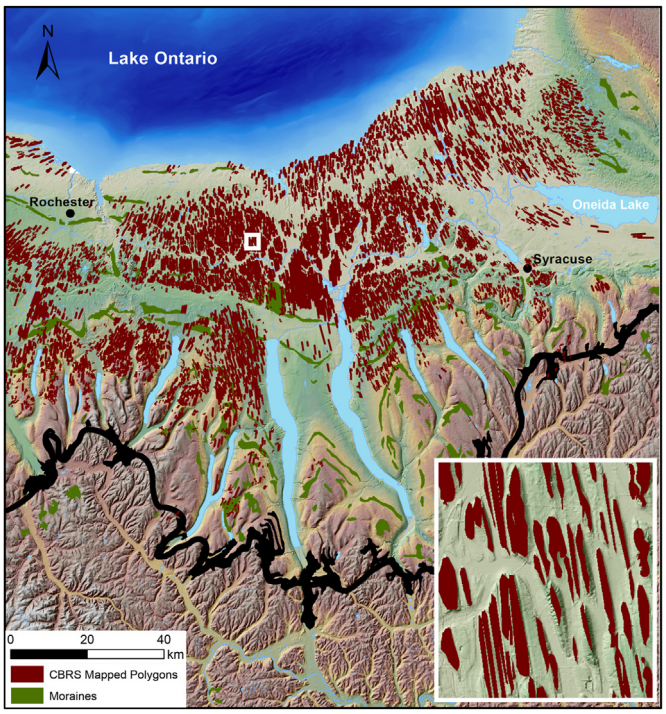

Fig. 5. Geomorphic map of study area generated from LiDAR DEM data with inset close-up showing mapping effectiveness. CBRS mapped polygons shown in maroon and moraine ridges manually mapped from hillshaded DEM shown in green. (For interpretation of the references to color in this figure legend, the reader is referred to the Web version of this article.)

orientation and elongation ratio) are tested individually since testing them together would imply a dependent relationship. While orientation and elongation ratio may be dependent on each other, this current method is not intended to directly explore that potential relationship. The Delaunay Triangulation method constrains groups to only include features in a group if at least one other group member is a natural neighbor. The GA algorithm used was Spatial "K" luster Analysis by Tree Edge Removal (SKATER) which uses a minimum spanning tree to find natural groupings in data (Lage et al., 2001). The minimum spanning tree was used to summarize both the spatial clustering and morphometric parameter similarity amongst the mapped bedforms and iteratively segment the bedforms into groups by using weighted edges that are proportional to the orientation or elongation ratio similarity of the bedforms it connects. GA was run with n_c set to 1–20 in ArcMap 10.7 as follows:

$$\frac{\left(\frac{R^2}{n_c-1}\right)}{\left(\frac{1-R^2}{n-n_c}\right)}$$

where:

$$R^2 = \frac{SST - SSE}{SST}$$

And *SST* is the between cluster differences and *SSE* reflects within cluster similarity:

$$SST = \sum_{i=1}^{n_c}\sum_{j=1}^{n_i}\left(V_{ij} - \overline{V}\right)^2$$

$$SSE = \sum_{i=1}^{n_c}\sum_{j=1}^{n_i}\left(V_{ij} - \overline{V_i}\right)^2$$

n_i = the number of landforms in cluster *i*.

V_{ij} = the value of the orientation or elongation ratio of the *j*th landform in the *i*th cluster.

$\overline{V}$ = the mean orientation or elongation ratio.

$\overline{V_i}$ = the mean orientation or elongation ratio in group *i*.

2.4.3. Measuring clustering effectiveness

Both K-Means and GA evaluate the potential for distinct clusters within the geomorphometric data. In order to determine the most statistically significant number of clusters in the data, both models need to be evaluated for their clustering effectiveness. This study used the Caliński-Harabasz pseudo F-statistic, which is a ratio reflecting within-cluster similarity and between-cluster difference (Caliński and Harabasz, 1974), to measure grouping effectiveness. For K-means clustering, the Caliński-Harabasz pseudo F-statistic values were calculated and the 'elbow method' was used to determine the most effective clustering. This was done in Python 3.7 using the *scikit-learn-yb* package with the *KelbowVisualizer* function. For GA, the clustering with the highest Caliński-Harabasz pseudo F-statistic calculated by the ArcMap 10.7 GA tool was determined to be the most effective. Once the clustering effectiveness was determined, summary statistics were calculated for both datasets and the clusters were mapped and displayed using ArcMap 10.7 and ArcScene 10.7. It is of note that the above method does not constrain uncertainty but instead measures the overall effectiveness of the clustering methods with the given data. Future research will explore methods for determining confidence intervals.

The following section describes in broad terms the principal results of the analyses described above which are then expanded on in the following sections in terms of paleoglaciology, bedform evolution and subglacial debris transport.

3. Results and interpretations

A total of 3690 individual bedforms were mapped as polygons, with an associated attribute table containing their length, width, elongation ratio, height, and orientation (Fig. 5).

3.1. Interpolation and clustering of bedform orientations

The Natural Neighbor interpolated surface generated from the calculated bedform orientations (Fig. 6) shows clear spatial differences in orientation, with the study area displaying a fan-like distribution of long-axis orientations ranging from almost 90° (measured clockwise from north) in the east to almost 270° in the west. It should however be noted that since the bedform orientations were interpolated independent to bedform spacing and abundance, the NN interpolated image does not take into consideration the fact that some parts of the study area contain few or no streamlined bedforms. Since the interpolation method does not inherently infer a dependent relationship between bedform spacing and orientation it is used here to illustrate evidence of distinct spatial clustering rather than an even gradation across the study area, suggesting the presence of discrete spatially-constrained flow units defined by orientation (example cluster

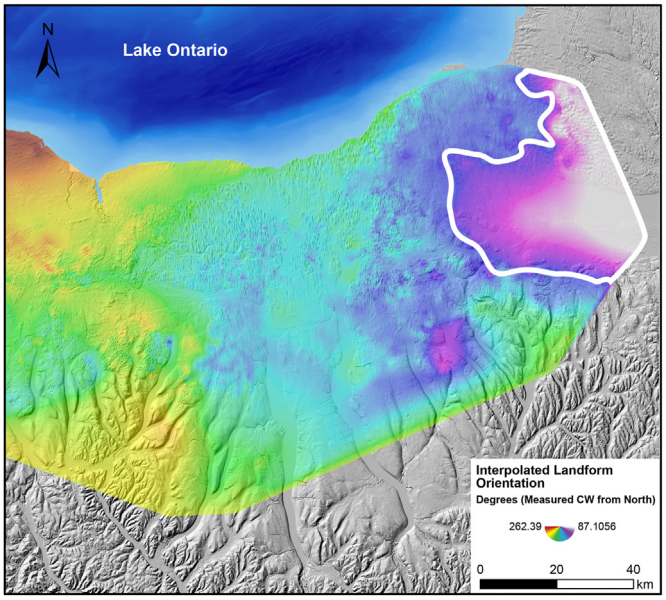

Fig. 6. Natural Neighbor interpolated raster surface generated from bedform orientations overlain on hill-shaded DEM. Orientations measured in degrees clockwise from north. Note the fan-like flow pattern with orientations ranging from ~90° to ~270° and the clustering of bedform orientations in the Finger Lake basin (example cluster outlined in white).

shown in Fig. 6). The subjective evidence of these flow units is not used to define their geographical extent but is an important diagnostic tool to determine whether spatially-constrained or non-spatially-constrained data clustering should be used. Consequently, the orientation data was clustered with the spatially-constrained GA algorithm to objectively assess whether the bed of the Seneca-Cayuga Ice Stream is characterized by multiple statistically distinct sub flow units. In this regard, GA was used on the CBRS mapped bedforms with 1–20 potential groupings tested, where a single (1) grouping would represent a single homogenous flow unit. The Caliński-Harabasz pseudo-F-statistic test was used to evaluate statistically evident number of flow units in the study area and found that the Seneca-Cayuga Ice Stream was complex and composed of eleven distinct sub flow units (Fig. 7; Table 1). These range in width from 15 to 50 km and together form the arcuate flow pattern in the Finger Lakes basins that is clearly seen in interpolated data (Fig. 8). The shape and extent of the flow units are approximately defined by individual lake basins which indicates that ice structure, flow direction and dynamics were strongly controlled by bedrock topography and the funneling of ice into lake basins.

3.1.1. Statistical exploration of flow velocity in each identified flow unit

Recently, several workers have drawn a qualitative relationship between bedform elongation and ice flow velocity (Margold et al., 2018; Barchyn et al., 2016; Ely et al., 2016; Eyles et al., 2016; Stokes and Clark, 2003; etc.), although this relationship among highly attenuated MSGLs under modern ice streams remains unclear (Holschuh et al., 2020). Since this study area contains both drumlins and MSGLs, the spatial distribution of elongation ratios of these bedforms within the eleven identified flow units (summarized in Table 1 and Figs. 6–8) suggests that ice flow velocity was not uniform across the former ice stream but varied from one flow unit to another. In this regard, evidence of fast ice flow is demonstrated by the presence of highly elongate bedforms (maximum elongation ratios of 13.81–89.82) within each set, but those flow units flowing directly into the basins of the Finger Lakes and the Oneida Lake basin have the highest mean elongation ratio, with the Seneca, Cayuga and Oneida basins showing the highest values along the central axis of the ice stream as a whole (Figs. 6 and 8). These are the largest and deepest basins indicating a strong topographic control on ice flow velocity within the lobe (see below). Also of note is that the identified flow units are reflected in the planform shape of the ice margin at the time of the VHM. The same observation can be identified for younger successive positions of the margin as it retreated northwards identified by moraine ridges which are segmented into loops that mark the terminus of each separate flow unit within the broader Seneca-Cayuga Ice Stream (Fig. 5).

The kurtosis and skewness of the elongation ratio values (Table 1) show that the distribution of elongation ratios in each of

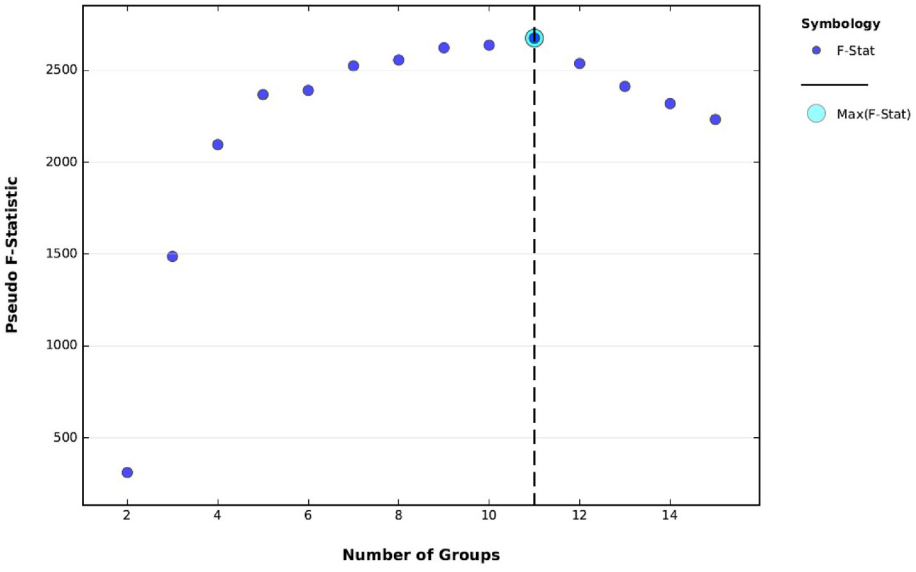

Fig. 7. The Caliński-Harabasz pseudo-F-statistic test results showing the optimal number of spatially constrained clusters of bedforms of varying orientation found in the data. Grouping effectiveness is measured as a ratio reflecting within-group similarity and between-group differences.

Table 1
Summary statistics of bedform elongation ratios within each flow unit identified from data clustering.

Flow-Set	Mean	Std. Err.	STd. Dev.	Variance	Kurtosis	Skewness	Range	Maximum	Count
1	3.90	0.31	4.01	16.11	13.60	3.40	28.36	29.07	169
2	12.79	1.37	5.31	28.23	−0.81	0.70	15.69	21.45	15
3	4.28	0.72	3.94	15.56	3.58	2.06	15.70	16.80	30
4	9.58	0.57	13.09	171.33	13.11	3.35	88.98	89.82	525
5	5.48	0.19	6.19	38.29	17.58	3.65	55.75	56.06	1056
6	3.69	0.25	3.61	13.01	12.78	3.37	23.96	24.56	213
7	5.49	0.81	7.50	56.22	18.97	3.91	50.78	51.47	88
8	5.80	0.36	5.90	34.86	9.12	2.60	39.22	39.79	273
9	6.56	0.22	6.63	44.00	10.40	2.80	51.10	51.63	924
10	7.07	0.52	8.23	67.78	14.33	3.02	69.02	69.69	255
11	6.75	0.50	6.01	36.13	2.87	1.77	27.25	28.16	142

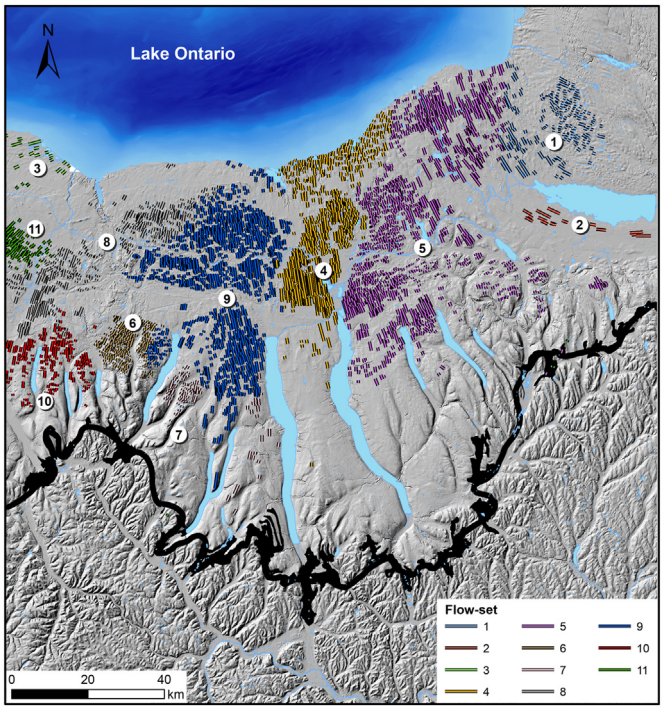

Fig. 8. LiDAR-generated geomorphic map of eleven statistically distinct ice flow unit clusters calculated using Grouping Analysis. The morphometrics of these flow units are summarized in Table 1.

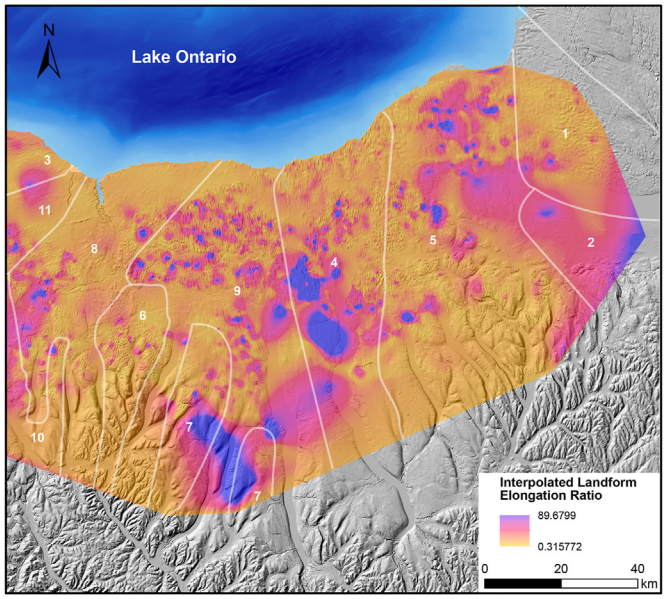

Fig. 9. Natural Neighbor interpolated raster surface generated from bedform elongation ratios overlain on hill-shaded DEM with previously calculated flow unit outlines in white. Note the increased elongation ratio near the Finger Lake basins and a gradient upglacier to less elongate bedforms on the southern shore of Lake Ontario, with variations of this gradient within each flow unit suggesting non-spatially controlled clustering. Also note the variability in elongation ratio within each flow unit with increased elongation in the flowline directly into the basins flanked by lower elongation flowlines.

the flow units are generally highly positively skewed (high skewness) with a high degree of peakedness (high kurtosis). This distribution suggests that the majority of highly elongate bedforms have a greater variance in elongation ratio (long tail in positive direction) that forms a gradient towards a predominance of less variable and relatively low elongation ratio bedforms (high peakedness). It can be noted in addition, that there is a high variability in the range and standard deviation of elongation ratios within each flow unit. This in flow unit variation can be explored further by interpolating the elongation ratio of the bedforms using Nearest Neighbor interpolation to constrain approximate ice flow velocity differences between each of the eleven statistically determined flow units.

3.2. Interpolation and clustering of bedform elongation ratios

The Natural Neighbor interpolated surface generated from the elongation ratios of the CBRS mapped bedforms (Fig. 9) shows clear spatial differences in elongation ratio, with the previously discussed flow units containing distinct patterns of elongation ratio distributions. The analysis reiterates the concentration of faster ice flow velocity towards the Finger Lake Basins, with the fastest velocities observed in the medial flowlines leading into the Keuka, Seneca, and Cayuga basins along the central axis of the Seneca-Cayuga ice stream as a whole. The interpolated surface also shows that these were flanked by bedforms that may be indicative of slower flow velocities. The horizontal distribution of ice flow velocity in each flow unit was qualitatively assessed from the interpolated surface and separated into three groups representing relative ice flow velocities: reduced flow velocity (mean elongation ratio of 3.9–5), intermediate flow velocity (5–7) and fast flow velocity (7+) (Fig. 10).

The Natural Neighbor raster image showed that, while the elongation ratios display a glaciologically significant distribution, there is little evidence of spatially controlled clustering since the interpolated raster contains repeated color intensity patterns that are not concentrated into geographic regions. This suggests that the study area contains non-spatially constrained clusters of

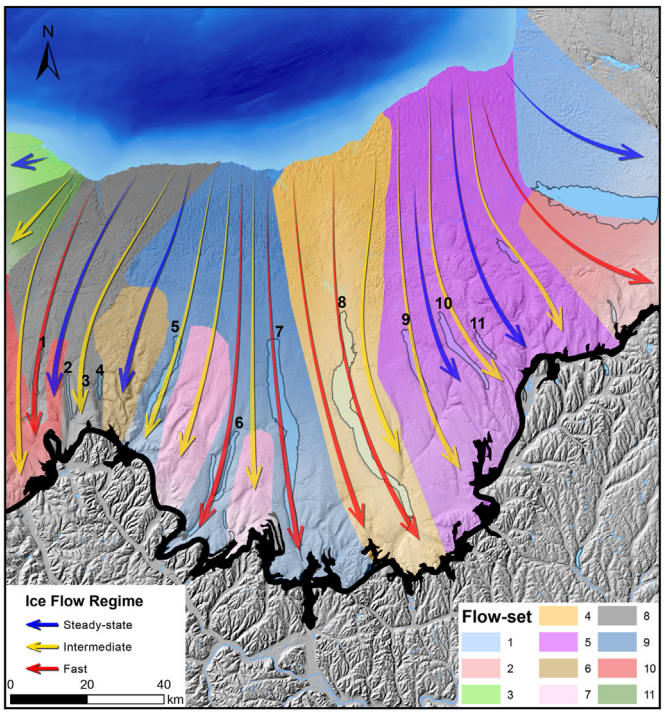

Fig. 10. Map showing the footprints of the eleven statistically validated ice flow unit groups determined using orientation Grouping Analysis. Ice flow directions shown with colors representing differences in ice flow velocity qualitatively estimated from elongation ratios of landforms along the flow line. Fastest flow units (#9 and 4) occur along the axes of the largest and deepest Finger Lakes basins (same basin numbering as in Fig. 2). (For interpretation of the references to color in this figure legend, the reader is referred to the Web version of this article.)

morphologically distinct bedforms. Previous studies commonly separate glacially streamlined bedforms into two non-spatially constrained clusters; drumlins and MSGLs using a breakpoint elongation ratio value ranging from 7 to 10 (e.g., Sookhan et al., 2016). Using a value of 7, a total of 932 bedforms are mapped as MSGLs (~25%) and the remaining 2758 as drumlins. However, analysis of high-resolution LiDAR data shows that this widely used binary separation of subglacial bedforms into drumlins and MSGLs using an elongation ratio value of 7–10 oversimplifies the full range of observed morphologies of bedforms and obscures the presence of continuums of bedforms such as recently described by Ely et al. (2016) and Eyles et al. (2016). The presence of continuums is clearly expressed geomorphologically southwards from Lake Ontario into the Finger Lakes, where drumlins narrow and become more elongated and progressively evolve into MSGLs. Of note is recognition of a specific intermediate streamlined morphotype first recognized and described as 'channeled' drumlins (named by Fairchild, 1900, 1907; 1911, 1929; Hubbard, 1906) which are drumlins cut longitudinally by single or several deep grooves thereby creating multiple more elongated streamlined ridges (Fig. 3). 'Channeled' or 'grooved' drumlins are in turn, transitional to MSGLs. Hart (1999) referred to these as 'complex drumlins' between what were described as 'equant drumlins' and 'flutes' and suggested this likely recorded an increase in ice velocity but did not recognize Fairchild's earlier work on this morphotype nor had access to high resolution topographic data that now reveals the full extent of grooving on the bed of the Seneca-Cayuga ice stream (Fig. 3).

Using the results of the CBRS bedform mapping the subglacial bedform continuum evident in New York State can now be resolved in much greater detail using non-spatially constrained data clustering for examining the distribution of elongation ratio among the broader population of streamlined bedforms. K-Means clustering was used to assess whether there are statistically distinct bedform morphotypes distributed throughout the study area, with 2–15 groupings evaluated using Caliński-Harabasz pseudo F-statistic test (Figs. 12 and 13). This method determined that the observed bedform continuum separates into seven statistically significant groups based on their elongation ratio (Fig. 13). The geographic distribution of these bedform morphotypes (Fig. 12) confirms the presence of distinct flow units of less elongate drumlin-dominated terrains near Lake Ontario that transition downglacier to more elongate bedform clusters concentrated in the Finger Lake basins. The seven bedform morphotypes illustrated in Fig. 13 capture and categorize the broad variety of streamlined subglacial bedforms in the study area and apparently elsewhere (e.g., Eyles et al., 2016, 2018) that can now be further quantitatively explored by further work on other streamlined beds and using other important metrics such as bedform relief and profile (e.g., Spagnolo et al., 2012).

3.3. Summary of results

The CBRS mapping tool mapped 3690 individual subglacially bedforms from the 170,000 km^2 of high-resolution DEM data prepared for the Finger Lakes region (Fig. 5). Data interpolation and clustering of the long-axis orientation of these bedforms showed that they form a fan-like distribution composed of some eleven spatially constrained and statistically distinct flow units outlined by the Finger Lakes basins (Fig. 8). If elongation ratio is used as a proxy for ice flow velocities, then interpolation and clustering of the bedform elongation ratios showed that ice flow velocities were highest in those flow units under ice flowing into the largest and deepest basins (Fig. 10). Furthermore, each of the flow units contain subglacial bedform continuums comprised of seven non-spatially constrained and statistically distinct bedform morphotypes (Fig. 11). These morphotypes are comprised of clusters of more elongate landforms in the narrow corridors of the Finger Lake basins with a diminishing abundance of elongate landforms upglacier towards Lake Ontario accompanying the change into channeled or grooved drumlins which in turn, are transitional to large equant drumlins on the southern shore of Lake Ontario (Figs. 9, 12 and 13).

The paleoglaciological significance of these results for understanding the flow of the Seneca-Cayuga Ice Stream, the evolution of subglacial bedforms and associated subglacial debris fluxes are explored in greater detail below.

4. Paleoglaciology of the Seneca-Cayuga ice stream

Sookhan et al. (2018a) identified and named the paleo Seneca-Cayuga Ice Stream with a width of some 80 km wide flowing south into the Finger Lakes from the overdeepened Rochester Basin cut into the floor of the Ontario Basin (Fig. 1). Results of a LiDAR based statistical analysis of subglacial bedforms described in the preceding sections now show that the ice stream was complex, consisting of a composite fan-shaped lobe that was structured into component flow units as much as 10 km wide, as a consequence of severe topographic confinement as ice was funneled southwards into deeply cut Finger Lake basins (see also Hess and Briner, 209). Chamberlin (1883) commented, in regard to the regional glaciation of the Finger Lakes, that 'ice flowed in streams' which is a clear reference to their very distinct morphology as a result of ice flow through narrow valleys. The glaciological structure of the broader ice stream may possibly have resembled modern ice streams in Antarctica that show a pronounced longitudinal 'striping' created by closely spaced flow units (see Glasser et al., 2015; Ely and Clark, 2016) though their origin is still not well understood. A simple

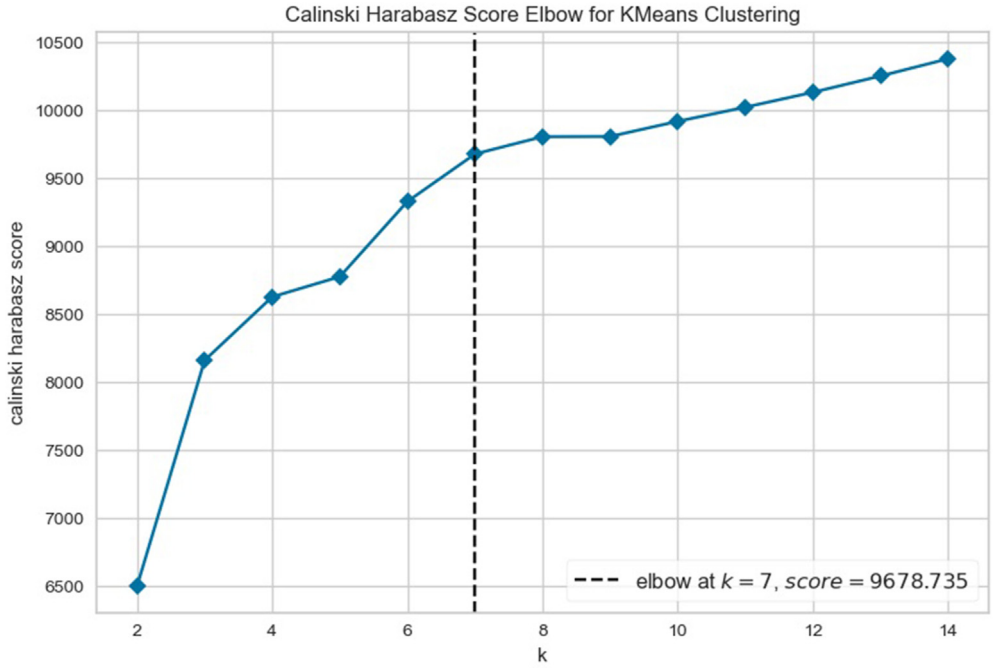

Fig. 11. The Caliński-Harabasz pseudo-F-statistic elbow test results showing the optimal number of clusters of bedforms based on K-Means analysis of their elongation ratios. Grouping effectiveness is measured as a ratio reflecting within-group similarity and between-group difference.

analogy may be made by reference to confluent ice flow units within valley glaciers reflecting contributions of ice from different sub-basins and classically reflected in the formation of medial moraines along the sutures of each flow unit (e.g., Eyles and Rogerson, 1977, 1978).

The conspicuous northward (i.e., upglacier) transition from mega-scale glacial lineations near the Finger Lakes into longitudinally dissected 'channeled' drumlins and in turn, into large equant drumlins in the north near Lake Ontario (Figs. 12–14, 15 ab) is seen on all flow units. This longitudinal variation in bedform type is interpreted as a record of increasing ice flow velocity toward the margin of each flow unit as a consequence of upglacier propagation of streaming flow from the terminus of each flow unit terminating in deep water (Fig. 16). This resulted in modification of an originally drumlinized bed produced under much lower ice flow velocities and the development of narrower, lower and more elongated bedforms under a faster flow regime (Fig. 13). Acceleration of ice flow velocity towards the ice margin can be ascribed to 'drawdown' of narrow ice tongues terminating in deep proglacial lakes trapped at the southern end of each basin. In this respect, Bloom (2018) described strand line elevations in the Cayuga and Seneca basins that indicate water depths as much as 600 m along the axis of the Seneca-Cayuga paleo ice stream (glacial Lake Newberry). The process of upglacier propagation of fast flow is known to be initiated at 'marine terminating' ice masses by rapid upstream migration of unstable grounding lines. Resulting fast flow then pulls out large volumes of ice from the interior of the ice sheet in response to rapid calving and draw down (e.g., Thomas, 1977; Hughes, 1987; Occhietti et al., 2001; Livingstone et al., 2012, 2016; Winsborrow et al., 2012; Livingstone and Clark, 2016). In this respect, it is highly significant that there is a very clear relationship between the subglacial geomorphology of each corridor and the depth and size of the Finger Lake basin into which it flowed. For example, the flow unit associated with the relatively shallow Canandaigua basin is immature (fewer MSGLs) compared to the larger and very much deeper Seneca and Cayuga basins which both record more extensive modification of drumlins in response to increased ice flow velocities resulting from the presence of deeper water bodies at their margin. (Fig. 10). In these flow units MSGLs extend much further upglacier of the terminus compared to other flow units

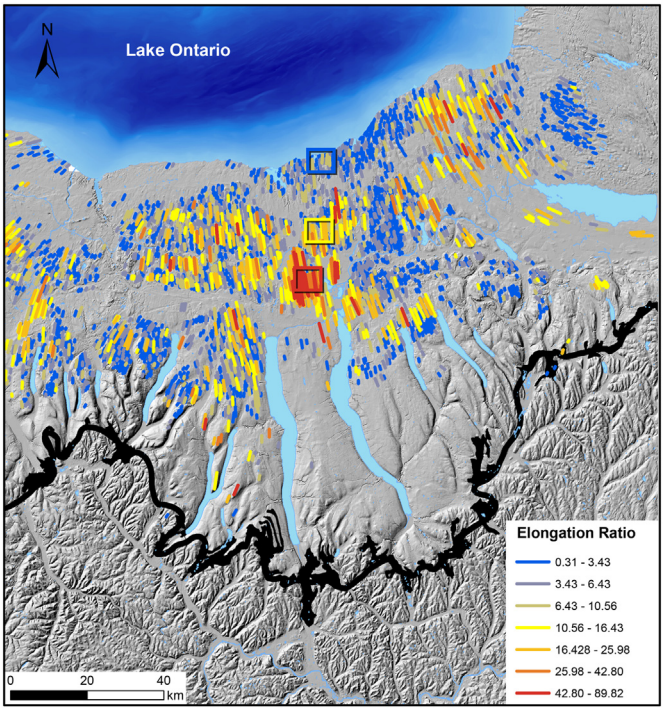

Fig. 12. Map showing the distribution of the seven K-Means clustering identified bedform morphotypes. Note the clustering of more elongate landforms in the narrow corridors of the Finger Lake basins and the diminishing abundance of elongate landforms upglacier towards Lake Ontario. Locations of Fig. 13 shown in insets.

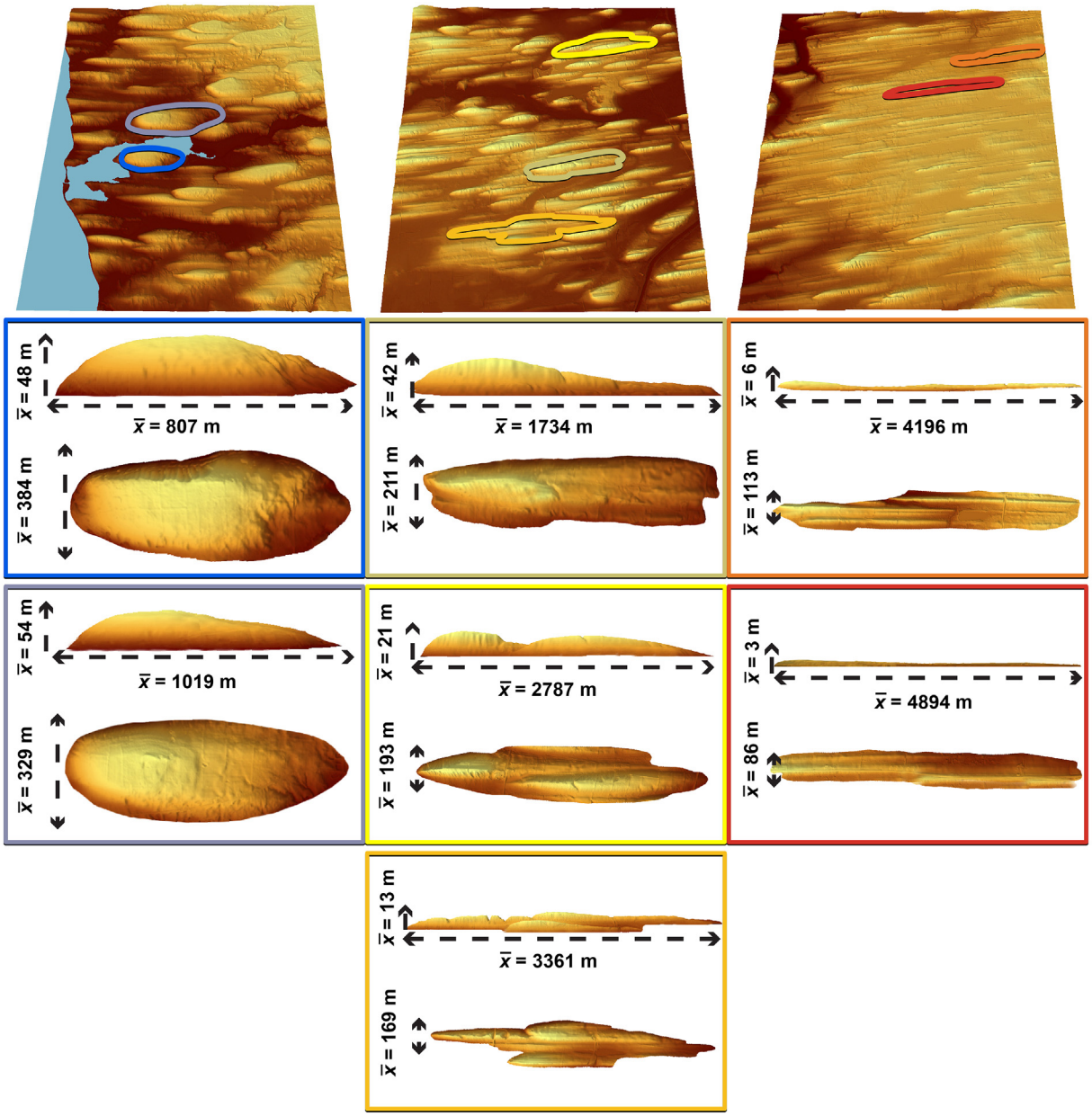

Fig. 13. 3D models showing geomorphology of the areas illustrated in Fig. 4 insets and characteristic intermediate bedforms of the continuum identified using K-Means clustering (drumlin in blues, channeled drumlins in yellows, and MSGLs in reds). Vertical exaggeration x5. The mean height, width and length of each continuum type is shown.

where the continuum of bedforms extends over much shorter distances (e.g., Fig. 16). This identifies a very strong control on ice flow dynamics by deep ice-frontal lakes.

5. Bedform evolution and subglacial debris flux

This is not the place for a lengthy review of the different hypotheses of subglacial bedform evolution but the data presented here identify a continuum of morphotypes between drumlins and MSGLs that is seen on the bed of multiple flow units within the Seneca-Cayuga Ice Stream. The continuum of subglacial bedforms (Figs. 3 and 13, 15 ab) is provisionally attributed to the progressive erosional lowering of large parent bedforms (drumlins) formed under preceding reduced flow velocities to more elongate bedforms under faster flowing ice. In this model, erosion accomplishes a reduction in overall relief amplitude of the bed, reducing basal drag and permitting faster ice flow across a grooved bed composed of mega-scale glacial lineations. Comparison of the seven bedform morphotypes present on the bed of the former Seneca-Cayuga ice stream (Fig. 13) shows that bedform height decreases as elongation increases which strongly suggests that the onset of fast flow is accompanied by significant bed lowering and a marked reduction in bed relief.

The upglacier (northern) part of each flow unit in New York State is dominated by large high standing equant-shaped drumlins (Miller, 1972; Hess and Briner, 2009). Near Lake Ontario, drumlin tops have been flattened by wave erosion in late glacial Lake Iroquois which formed after 12,500 ybp in the Ontario Basin (e.g., Slater, 1929; Francek, 1991; Rayburn et al., 2005, 2011; Bird and Kozlowski, 2016; Zaremba and Scholz, 2019) but their form is still distinct. Stratigraphic investigations along coastal outcrops through drumlin cores suggests that they are subglacially streamlined

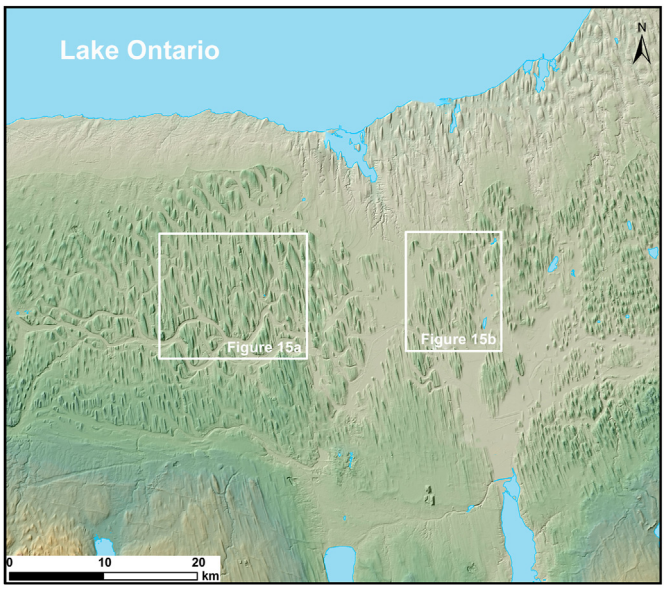

Fig. 14. 'Transition zone' on the bed of the paleo- Seneca-Cayuga Ice Stream showing upstream (northwards) propagation of bedform elongation from MSGLs to dissected or 'channeled' drumlins to large drumlins near Lake Ontario. For detailed images see Fig. 15 A, B.

islands or 'outliers' of previously thick antecedent drift including tills and outwash, supporting an erosional origin for these bedforms (see Gravenor, 1953, 1957; White, 1985; Boyce and Eyles, 1991; Kerr and Eyles, 2007; Ó Cofaigh et al., 2010, 2013; Sookhan et al., 2018a, b). Furthermore, bedrock-cut mega-scale glacial lineations are in fact, very common in Southern Ontario and New York State (White, 1985; Muller and Cadwell, 1986; Isachsen et al., 2000; Eyles, 2012; Eyles and Doughty, 2016; Krabbendam et al., 2016; Sookhan et al., 2018a, b; Bukhari et al., 2021). Alternatively, the observed inverse relationship between bedform height and elongation may be the result of changes in sediment volume available for deposition. As such, the results of this study highlight the significance of further exploring the relationship between the now statistically determined bedform continuum and subglacially streamlined bedform evolution to determine the relative roles of erosion, deposition, or combinations of the two (e.g., Fowler, 2000, 2018; Stokes et al., 2013; Eyles et al., 2016; Iverson et al., 2017). This needs to be combined with further analysis of the geology of these bedforms though much work has already been accomplished in this regard (see literature reviews in Stokes et al., 2013 and Eyles et al., 2016).

Evidence of the predominance of erosion under the Seneca-Cayuga Ice Stream is supported by seismic reflection data on the glacial sedimentary fills of the Finger Lake basins through which ice flowed (Mullins et al., 1996). High resolution marine seismic reflection data from these lakes show that any pre-existing sediment fill was entirely removed during southward ice flow to the VHM and that each basin was subsequently backfilled during ice retreat with as much as 250 m of glaciolacustrine sediment during a single phase of sedimentation. The same history of deep erosion of pre-existing sediment to bedrock followed by backfilling during deglaciation is apparent from deep drilling at Canandaigua Lake (Wellner et al., 1996) and appears to be typical of other deep 'fiord lakes' in western North America where as much as 100 m of sediment was rapidly deposited following complete removal of pre-existing sediment fills down to bedrock below fast flowing ice (e.g., Eyles et al., 1990, 1991; Mullins et al., 1991; see also Smith et al., 2012). The confined bedrock basins of the Finger Lake basins functioned essentially as subglacial tunnel valleys discharging subglacial sediment and water south to the VHM (Bloom, 2018). In this regard, the sedimentology and stratigraphy of VHM and its overall depositional and paleoglaciological context, invites further detailed comparison with large ice-proximal subaqueous-deposited sediment accumulations ('morainal banks') built at the terminus of marine-terminating ice streams (e.g., Dowdeswell et al., 2012; 2015, 2016). The very large volume of this depositional system and the limited time frame for fast ice flow in the Finger Lakes region (see above) identifies accelerated subglacial erosion of rock and sediment by glacial abrasion and subglacial meltwaters below fast flowing which removed any pre-existing sediment fill and thus exposed jointed, easily quarried Paleozoic carbonates and soft shales to intense subglacial scouring.

A highly illustrative record of enhanced transport of subglacial debris below the Seneca-Cayuga Ice Stream is retained in the regional petrography of Finger Lake tills (Holmes, 1952). A narrow west-east oriented outcrop belt of distinctive Silurian Oswego and Albion ('Medina') sandstones extends west-east for some 60 km along the Lake Ontario shoreline (Fig. 17). This belt acted as a well-defined 'line source' of subglacially-eroded debris being transported southwards ice flowing out of the deep Rochester Basin into the Finger Lakes. Red and green-colored quartzites of the Silurian Grimsby Formation are a very conspicuous component of surface tills within channeled drumlins and MSGLs as far south as the VHM some 100 km south of the outcrop belt. Holmes (1952) identified a progressive reduction from large locally derived bedding-plane bedrock slabs of quartzite near Lake Ontario to granules near VHM attributed to extended subglacial transport and comminution. He also showed that the distance of transport of quartzites (specifically as clasts 6.3–12.6 mm in diameter) is markedly non-uniform across the Finger Lakes region and surrounding parts of the Allegheny Plateau and had been carried further in basins compared to interfluve areas.

Holmes' quantitative dataset and map were digitized in the present study, georectified and superposed onto the LiDAR digital elevation model of the Finger Lakes area. The resulting isopleth map (Fig. 17) shows a very distinct finger-like dispersal train consisting of ribbons of quartzite-bearing till. These occur in tills along each flow unit of channeled drumlins and MSGLs left by flow units within the composite Seneca-Cayuga Ice Stream. This pattern is consistent with enhanced southward transport of debris and included quartzite marker clasts across the bed of each individual flow unit. Moreover, the considerable length of the dispersal train in each flow unit (as much 110 km) contrasts greatly with the more limited distance of transport (~70 km) of the same detrital quartzite present in tills in ice stream interfluve areas on the surrounding Allegheny Plateau where ice flow velocity was likely much reduced (Fig. 10). It is noteworthy that Mesozoic diamond-bearing kimberlites occur in the Finger Lakes region (e.g., Van Fossen and Kent, 1993; Bailey and Lupulescu, 2015) and, more broadly, the paleoglaciology of the region and recognition of separate flow units identified here is of much interest to mineral explorationists now working with the implications of the emerging 'ice stream paradigm' (e.g., Paulen et al., 2017; Boswell et al., 2018; McClenaghan et al., 2018). The distinctive 'finger-like' distribution pattern of quartzites in upper New York State tills (Figs. 16 and 17) confirms the composite structure of the Seneca-Cayuga Ice Stream and is markedly different from classical dispersal trains produced under reduced ice flow velocities which typically, take the much simpler form of a broad dispersal fans (see Brigham, 1894; DiLabio, 1990; McClenaghan and Paulen, 2017; Boswell et al., 2018). The data presented herein from the Finger Lakes in regard to debris transport below a paleo ice stream, warrant further examination of the

beds of other paleo ice streams associated with areas of bedrock mineralisation such as on the Canadian Shield to identify the role of narrow subunits within the broader ice stream in moving debris over enhanced distances of transport. This aspect begs the question as to the time frame of fast flow and this is briefly examined in the next section.

6. Duration of fast flow and rate of bedform evolution

The identification of well-defined statistically validated flow units of drumlins-MSGL continuums in upper New York State is unambiguous evidence of topographically controlled fast ice flow southwards through the Finger Lake basins to the VHM. Notably, MSGLs cannot be recognized to the south of the moraine system indicating that VHM marks a major regional change in ice flow dynamics within the eastern Great Lakes sector of LIS. VHM is correlated with the Lake Escarpment Moraine in Pennsylvania (Shepps et al., 1959; Braun, 2004), the Defiance Moraine in Ohio (Eschman, 1985), the Paris and Galt Moraines in Southern Ontario (Barnett, 1979) and the prominent Middleburg Readvance in the Mohawk-Hudson river valleys and the Charleston Moraine, considered to mark the position of the LIS margin sometime between ~14.8 and 13.6 ka (most likely ~14.4 ka; Ridge, 2003, 2004; Ridge et al., 1991, 2012; Fullerton, 1986; Muller and Calkin, 1993; Mullins et al., 1996; Millar, 2004; Franzi et al., 2016; Bloom, 2018). It is thus evident that VHM records the change from regional flow of the LIS to much more localized topographically-controlled fast flow marked by topographically controlled ice streams. Ross et al. (2006) recognized the geomorphic record of an abrupt change in ice flow at the same time along the St. Lawrence Valley just east and north of the present study area, involving the onset of fast flow both into the Ontario Basin coeval with the onset of a large St. Lawrence Valley Ice Stream flowing east to the Gulf of St. Lawrence (Carl, 1978; Occhietti et al., 2001; Ross et al., 2009, 2011). This marked change in the glaciology and mode of flow of the LIS margin broadly coincides with the abrupt beginning of the short-lived Bølling-Allerød warming event sometime between 14,600 and 14,100 ka (Clark et al., 2001; Rasmussen et al., 2006) which is associated with Meltwater Pulse 1 A when global sea level rose ~ 20 m in less than 500 years (Anderson and Lewis, 1985; Deschamps et al., 2012). At this time, LIS was undergoing rapid melting and thinning with a large length of its margin terminating in deep water. This phase was likely very short-lived.

The St. Lawrence Ice Stream shut down between c.14.0 to 13.9 ka (Occhietti et al., 2001) and the Ontario Basin was partially deglaciated by 13.3 ka during what has in some quarters been termed the Mackinaw Interstadial (Barnett, 1992) though a simple climatic control on ice flow and ice margin positions is considered extremely unlikely within the Great Lake basin given the considerable influence of topography and deep ice marginal lakes on ice margin form, behaviour and flow. A subsequent short-lived reorganisation and resurgence of the LIS at c. 13.0 ka in the form of the Halton Ice Stream out of the Ontario basin to abut the south-flowing Simcoe Ice Stream (Taylor, 1913; Sookhan et al., 2019). Thereafter, ice in the Ontario Basin retreated rapidly eastward out of the basin by calving into glacial Lake Iroquois (Bukhari et al., 2021). The basin was ice-free and glacial Lake Iroquois had drained by at least 12.25 ka (Blewett et al., 1993; Dyke et al., 2002; Dyke, 2004; Donnelly et al., 2005; Margold et al., 2018).

A much more detailed analysis of the timing and rate of bedform evolution is in preparation but at this stage but at this point the above synthesis of available age dates indicates that duration of fast ice flow in New York State was very short and likely limited to a few hundred years. In turn, this estimate provides valuable constraints on the time available for the formation of morphotypes from

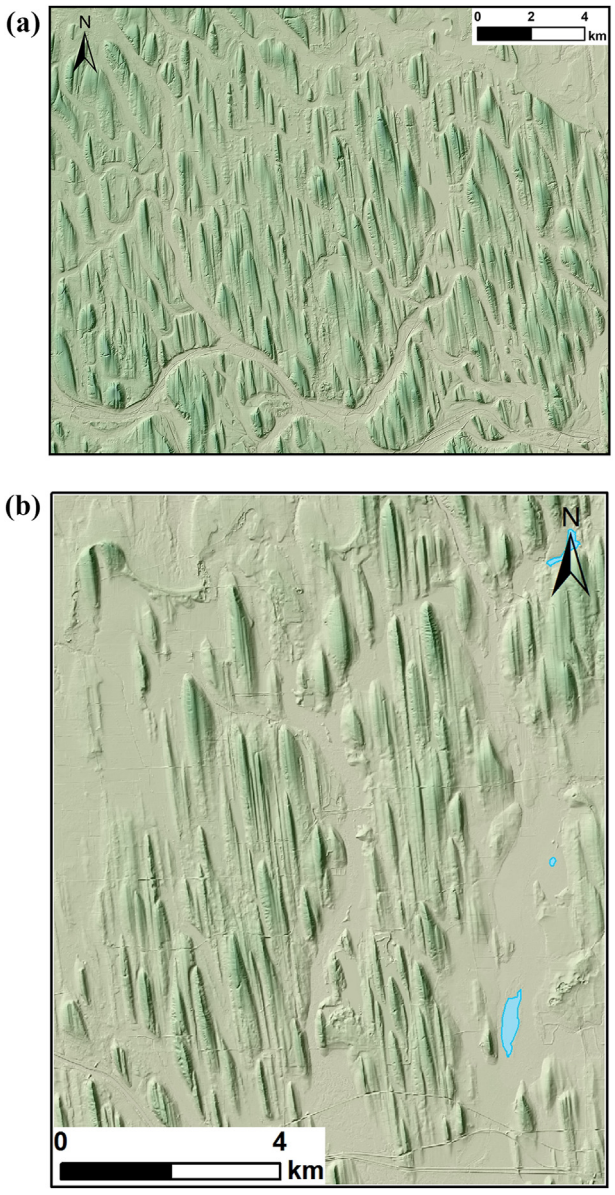

Fig. 15. A and B: Examples of 'channeled' drumlins that are transitional from drumlins to MSGLs. Vertical exaggeration x 5.

drumlins to channeled drumlins and MSGLs under fast flowing ice (Figs. 13 and 15a,b). Rapid bedform evolution is suggested. It can be speculated that parent drumlins evolved under a much longer time frame under an earlier ice flow regime as the Laurentide Ice Sheet expanded and entered New York State. The streamlined bed of the Seneca-Cayuga Ice Stream immediately north of the Finger Lakes is crossed obliquely by several till-cored end moraines (e.g., Goldthwait, 1922, Fairchild, 1932; Goldthwait et al., 1965; Miller, 1974; Krall, 1977; Ridky and Bindschadler, 1990; Millar, 2004, Fig. 1). These record punctuated recession of the ice margin involving short-lived still stands of the ice front the Seneca-Cayuga Ice Stream withdrew from deep lake bodies in each basin. It seems likely that debris eroded from the bed to lower overall bed relief (Figs. 13 and 15 ab) was advected toward the ice margin to accumulate either as frontal moraines or was moved within the confines of narrow lake basins to the ice margin to be deposited as subaqueous outwash of the VHM. The repeated still stands recorded north of the Finger Lakes are consistent with the termination of fast

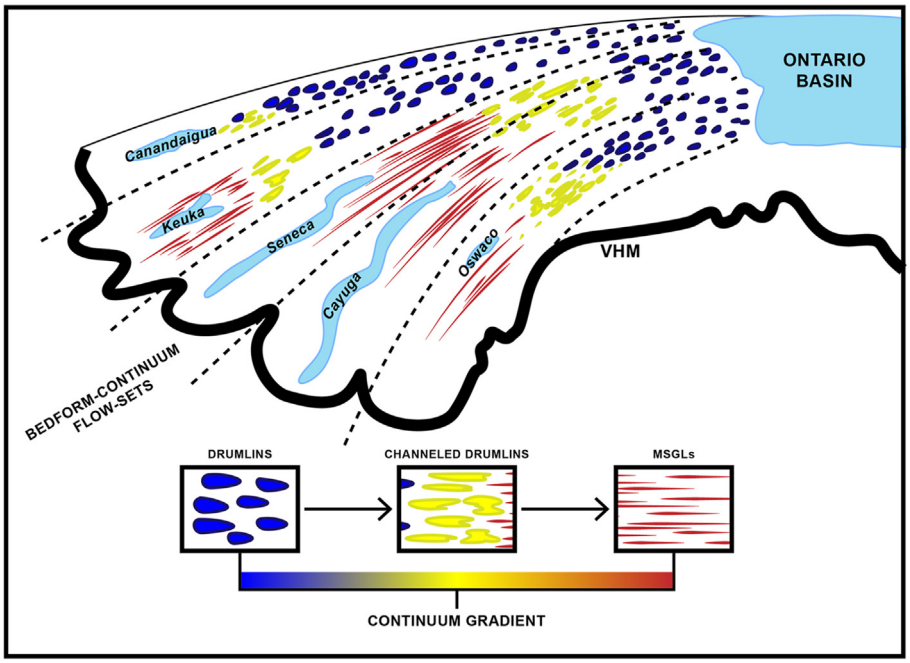

Fig. 16. Simplified conceptual model showing the upstream propagation of MSGLs as ice streaming develops in the Finger Lakes region.

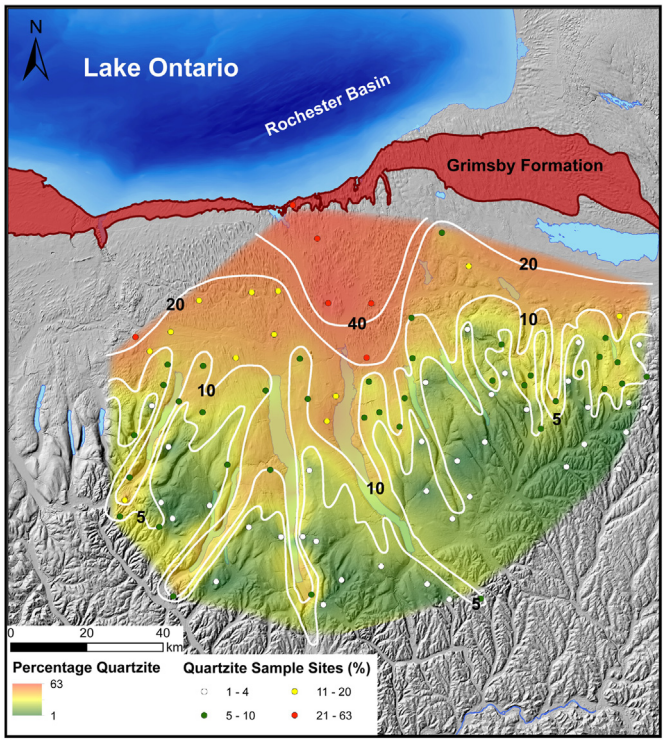

Fig. 17. Distribution and percentage of red and green quartzite clasts (6.3–12.6 mm in diameter) of the Paleozoic Grimsby Formation in Finger Lake ice-stream tills derived from linear west-east oriented outcrop area immediately south of Lake Ontario. Original lithologic data from Holmes (1952) was georectified and placed on LiDAR-generated geomorphic map of subglacial bedforms (Fig. 3). Note enhanced subglacial transport of quartzite by ice streams occupying Finger Lake basins (same basin numbering as in Fig. 2). (For interpretation of the references to color in this figure legend, the reader is referred to the Web version of this article.)

flow as ice retreated northwards out of the Finger Lakes beyond the destabilizing influence of deep water.

7. Discussion

This paper presents a systematic approach for the statistical examination of subglacial streamlined bedforms left by former mid-latitude ice sheets from LiDAR-based high-resolution topographic data. This exercise demonstrates that significant paleoglaciological information on the structure and mode of flow of ancient ice lobes can be determined from the spatial distribution of changing bedforms both perpendicular and parallel to ice flow. The analysis outlined herein reveals a much richer assemblage of subglacial bedforms than hitherto recognized in the literature and thus questions the practice of using a simple binary division of lineation populations into drumlins and mega-scale glacial lineations based on an arbitrary value of elongation ratio. Several authors have suggested the presence of subglacial continuums in subglacial bedforms (e.g., Aario, 1977; Rose, 1987; Ely et al., 2016) and Eyles et al. (2016) illustrated intermediate morphotypes between drumlins and MSGLs. The present paper takes this analysis further by showing how statistically determined clusters in bedform morphological data identifies the presence and shapes of intermediate streamlined morphotypes such as previously recognized 'channeled drumlins.' The key step in this progress has been having access to high resolution LiDAR topographic data sets (Figs. 3, 12 and 13). The quantitative methodology presented here now provides an objective approach to subdividing streamlined bedforms into statistically similar clusters of morphotypes using multivariate or unsupervised clustering and is a necessary first step towards ultimately adopting a machine learning approach for quantifying paleo ice sheet behaviour from analysis of their beds.

The structure of the composite Seneca-Cayuga Ice Stream that flowed into the glacially-overdeepened Finger Lakes basins of Upper New York State sometime after c. 14.5 ka is recorded geomorphologically by statistically significant flow units of drumlins and mega-scale glacial lineations and transitional 'channelled drumlin' morphotypes. This structure is the product of regional ice

flow that was severely constrained by the topography of over-deepened lake basins cut into the northern edge of the Allegheny Plateau. The same analysis also identifies faster axial flow and slow flow along the margins of each flow unit recording frictional retardation along their margins as is well known in modern composite glaciers (Fig. 10). At this point in time, it is unclear whether each stage in the bedform continuum (drumlins, channeled drumlins, MSGLs) is the geomorphic response to a uniform increase in ice flow velocity from steady state (<~250 m yr?) to streaming flow (>1000 m yr) or may record incremental jumps in velocity akin to those seen in fluvial systems. Enhanced subglacial transport of debris at the base of each flow unit is expressed as narrow plumes of till containing detrital quartzite sourced from a narrow west-east oriented outcrop belt of Paleozoic strata. A dominantly erosional subglacial regime below Finger Lakes ice streams is supported by the absence of any pre-existing sediment fill in the lake basins, the depth of their bedrock floors below mean sea level and the deposition of a large high-volume morainal system (VHM) at the southern end of each trough. The role of fast flow and rapid glacial excavation of soft rock by ice streams in excavating the Finger Lake basins as suggested by Mullins and Hinchey (1989) now looks very likely, perhaps solving long standing questions as to the origin of these intriguing basins.

8. Conclusions

Deriving paleoglaciological information from the geomorphology of ancient ice sheets beds is a key objective of much current research by glacial geologists. To this end, the present study has outlined a quantitative objective methodology for describing the shape of subglacially-streamlined bedforms from high resolution LIDAR-based data sets on the bed of ancient ice sheets.

Specifically, this paper has

1: Identified the importance of bedrock topography in controlling the number of flow units within an ancient ice stream and the key role played by deep ice marginal water bodies in triggering fast ice flow that propagated upglacier resulting in rapid alteration of pre-existing streamlined bedforms.

2: Revealed the existence of statistically validated transitional morphotypes between drumlin and mega-scale glacial lineation 'end members'. Previous workers have broadly suggested the existence of such continuums but this is the first study to clearly and specifically identify their shape and form which is a significant step forward. It must be stressed however, that future work may well expand the number of morphotypes and also needs to integrate such work with the formation of non-streamlined subglacial beds (e.g., 'till plains') together with the geology and composition of each morphotype. The bedform continuum recognized herein is provisionally linked to erosion and lowering of an originally drumlinized bed in response to an increase in ice flow velocity, though other explanations need to be explored.

3: Shown that morphotype mapping using the methodology presented here, provides a valuable tool for determining the overall paleoglaciological structure of ancient ice lobes and with further work and analysis, will eventually allow reconstruction of paleo ice flow velocities and inferred basal drag conditions along and across component ice flow units.

4: Provided a provisional time frame for the evolution of subglacial bedforms that suggests that mega-scale glacial lineations evolve from parent drumlins in a few hundred years, with major implications for quantifying subglacial debris fluxes and for mineral exploration studies.

Author statement

Shane Sookhan: Conceptualization, Methodology, Data curation, Writing – original draft, Writing – review & editing, Visualization; Nick Eyles: Supervision, Writing – original draft, Writing – review & editing, Resources, Investigation; Syed Bukhari: Methodology, Visualization; Roger Paulen: Investigation, Validation

Declaration of competing interest

The authors declare that they have no conflict of interest.

Acknowledgements

Field and laboratory work was funded by the Natural Sciences and Environmental Research Council of Canada (NE), the Province of Ontario (SS) and the Geological Survey of Canada's Geo-Mapping for Energy and Minerals (GEM) Program (RP; NRCan contribution number 20200707). An earlier version of this manuscript benefitted from a meticulous review by Stephen. Wolfe (Geological Survey of Canada). We also thank Matteo Spagnolo and Jeremy Ely for their many helpful comments during the review process.

References

Aario, R., 1977. Classification and terminology of morainic landforms in Finland. Boreas 6 (2), 87–100.
Anderson, T.W., Lewis, C.F.M., 1985. Postglacial water-level history of the Lake Ontario basin. In: Karrow, P.F., Calkin, P.E. (Eds.), Quaternary Evolution of the Great Lakes, vol. 30. Geological Association of Canada, Special Paper, pp. 231–253.
Bailey, D.G., Lupulescu, M.V., 2015. Spatial, temporal and compositional variation in Mesozoic kimberlites in New York State. Lithos 212–215, 298–310.
Barchyn, T.E., Dowling, T.P.F., Stokes, C.R., Hugenholtz, C.G., 2016. Subglacial bedform morphology controlled by ice speed and sediment thickness. Geophys. Res. Lett. 43, 7572–7580.
Barnett, P.J., 1979. Glacial Lake Whittlesey: the probable ice frontal position in the eastern end of the Erie Basin. Can. J. Earth Sci. 16, 568–574.
Barnett, P.J., 1992. Quaternary geology of Ontario. In: Geology of Ontario. Ontario Geological Survey, Special, vol. 4, pp. 1011–1088.
Bird, B., Kozlowski, A., 2016. Late Quaternary Reconstruction of Lake Iroquois in the Ontario Basin of New York, vol. 80. N. Y. State Mus. Map & Chart.
Blewett, W.L., Winters, H.A., Rieck, R., 1993. New age control on the port huron moraine in northern Michigan. Phys. Geogr. 14, 131–138.
Bloom, A.L., 2018. Gorges History. Landscapes and Geology of the Finger Lakes Region. Paleontological Research Institution, Ithaca, New York.
Boswell, S.M., Toucanne, S., Creyts, T.T., Hemming, S.R., 2018. Continental-scale transport of sediments b y the Baltic Ice Stream elucidated by coupled grain size and Nd provenance analyses. Earth Planet Sci. Lett. 490, 143–150.
Boyce, J.I., Eyles, N., 1991. Drumlins carved by deforming till streams below the Laurentide ice sheet. Geol. 19, 787–790.
Braun, D.D., 2004. Glaciation of Pennsylvania, USA. In: Ehlers, J., Gibbard, P.L. (Eds.), Quaternary Glaciations – Extent and Chronology, Part II. Elsevier, Amsterdam, pp. 237–242.
Briner, J.P., 2007. Supporting evidence from the New York Drumlin Field that elongate subglacial bedforms indicate fast ice flow. Boreas 36, 143–147.
Brigham, A.P., 1894. Drift boulders in central New York. Am. J. Sci. 149, 213–228.
Bukhari, S., Eyles, N., Sookhan, S., Paulen, R., Krabbendam, M., Putkinen, N., 2021. Regional subglacial quarrying and abrasion below a paleo ice stream crossing the Shield-Paleozoic boundary of central Canada: the importance of substrate control. Boreas in press.
Cadwell, D.H., Muller, E.H., 2004. New York glacial geology, U.S.A. In: Ehlers, J., Gibbard, P.L. (Eds.), Quaternary Glaciations –Extent and Chronology, Part II. Elsevier, Amsterdam, pp. 201–205.
Caliński, T., Harabasz, J., 1974. A dendrite method for cluster analysis. Commun. Stat. Theor. Methods 3 (1), 1–27.
Carl, J.D., 1978. Ribbed moraine-drumlin transition belt, St. Lawrence Valley. Geol. 6, 562–566. New York.
Chamberlin, T.C., 1883. Terminal moraine of the second glacial epoch. Third Ann. Rep. US Geol. Surv 353.
Clark, P.U., Marshall, S.J., Clarke, G.K.C., Hostetler, S.W., Licciardi, J.M., Teller, J.T., 2001. Freshwater forcing of abrupt climate change during the last glaciation. Sci 293, 283–287.
Clayton, K.M., 1965. Glacial erosion in the Finger Lakes region (New York State, USA). Geomorphology 9, 50–62.
Clayton, L., 1972. Glacial Erosion in the Finger Lakes Region, New York State. In: Embleton, C. (Ed.), Glaciers and Glacial Erosion. Palgrave, London, pp. 173–187.

Coates, D.R., 1974. Reappraisal of the glaciated Appalachian Plateau. In: Coates, D.R. (Ed.), Glacial Geomorphology. State University of New York, Binghamton, NY, pp. 205–244.
Deschamps, P., Durand, N., Bard, E., Hamelin, B., Camoin, G., Thomas, A.L., Henderson, G.M., Okuno, J., Yokoyama, Y., 2012. Ice-sheet collapse and sea-level rise at the Bølling warming 14,600 years ago. Nat 483, 559–564.
DiLabio, R.N.W., 1990. Glacial dispersal trains. In: Kujansuu, R., Saarnisto, M. (Eds.), Glacial Indicator Tracing. A.A. Balkema, Rotterdam, pp. 109–122.
Donnelly, J.P., Driscoll, N.W., Uchupi, E., Keigwin, L.D., Schwab, W.C., Thieler, E.R., Swift, S.A., 2005. Catastrophic meltwater discharge down the Hudson Valley: A potential trigger for the Intra-Allerød cold period. Geol. 33, 89–92.
Dowdeswell, J.A., Hogan, K.A., Arnold, N.S., Mugford, R.I., Wells, M., Hirst, J.P., Decalf, C., 2015. Sediment rich meltwater plumes and ice proximal fans at the margins of modern and ancient tidewater glaciers: Observations and modelling. Sedimentology 62, 1665–1692.
Atlas of submarine Glacial Landforms, Modern, Quaternary and Ancient. In: Dowdeswell, J.A., Canals, M., Jakobsson, M., Todd, B.J., Dowdeswell, E.K., Hogan, K.A. (Eds.), Geological Society of London Memoir 46, 316.
Dowling, T.P., Spagnolo, M., Möller, P., 2015. Morphometry and core type of streamlined bedforms in southern Sweden from high resolution LiDAR. Geomorphology 236, 54–63.
Dyke, A.S., 2004. An outline of North American deglaciation with emphasis on central and northern Canada. In: Ehlers, J., Gibbard, P.L. (Eds.), Quaternary Glaciations – Extent and Chronology, Part II. Elsevier, Amsterdam, pp. 373–424.
Dyke, A.S., Andrews, J.T., Clark, P.U., England, J.H., Miller, G.H., Shaw, J., Veillette, J.J., 2002. The Laurentide and Innuitian ice sheets during the last glacial maximum. Quat. Sci. Rev. 21, 9–68.
Ely, J.C., Clark, C.D., 2016. Flow-stripes and foliations of the Antarctic Ice Sheet. J. Maps 12, 249–259.
Ely, J.C., Clark, C.D., Spagnolo, M., Stokes, C.R., Greenwood, S.L., Hughes, A.L.C., Dunlop, P., Hess, D., 2016. Do subglacial bedforms comprise a size and shape continuum? Geomorphology 257, 108–119.
Eschman, D.F., 1985. Summary of the Quaternary History of Michigan, Ohio and Indiana. J. Geol. Educ. 33, 161–167.
Evans, D.J.A., Young, N.J.P., Ó Cofaigh, C., 2014. Glacial geomorphology of terrestrial-terminating fast flow lobes/ice stream margins in the southwest Laurentide Ice Sheet. Geomorphology 204, 86–113.
Eyles, N., 2012. Glacially cut rock drumlins and megagrooves of the Niagara Escarpment, Ontario, Canada cut below the Saginaw-Huron Ice Stream. Quat. Sci. Rev. 55, 34–49.
Eyles, N., Rogerson, R.J., 1978. A framework for the investigation of medial moraine formation; Austerdalsbreen, Norway and Berendon Glacier, British Columbia. J. Glaciol. 20, 99–114.
Eyles, N., Rogerson, R.J., 1977. Glacier movement, ice structures and medial moraine from at a glacier confluence, Berendon Glacier, British Columbia, Canada. Can. J. Earth Sci. 14, 2807–2816.
Eyles, N., Mullins, H.T., Hine, A., 1990. Thick and fast; sedimentation in a Pleistocene fiord-lake basin. British Columbia, Canada. Geol. 18, 1153–1157.
Eyles, N., Mullins, H.T., Hine, A., 1991. The seismic stratigraphy of Okanagan Lake, British Columbia; a record of rapid deglaciation in a deep 'fiord-lake' basin. Sediment. Geol. 73, 13–41.
Eyles, N., Doughty, M., 2016. Glacially streamlined hard and soft beds of the paleo-Ontario Ice Stream in central Canada. Sediment. Geol. 338, 51–71.
Eyles, N., Putkinen, N., Sookhan, S., Arbelaez-Moreno, L., 2016. Erosional origin of drumlins and megaridges. Sediment. Geol. 338, 2–23.
Eyles, N., Arbelaez-Moreno, L., Sookhan, S., 2018. Ice streams within the last Cordilleran Ice Sheet of western North America. Quat. Sci. Rev. 179, 87–122.
Faber, V., 1994. Clustering and the continuous k-means algorithm. Los Alamos Sci. 22, 138–144.
Fairchild, H.L., 1900. A channeled drumlin (Abstract). Sci. XI, No 264, 104.
Fairchild, H.L., 1907. Drumlins of central western New York. N. Y. State Mus. Bull. 3, 391–443.
Fairchild, H.L., 1911. Radiation of glacial flow as a factor in drumlin formation. Geol. Soc. Am. Bull. 22, 734.
Fairchild, H.L., 1929. New York drumlins. Rochester Acad. Sci. Proc. 7, 1–37.
Fairchild, H.L., 1932. New York moraines. Geol. Soc. Am. Bull. 43, 627–662.
Fowler, A.C., 2000. An instability mechanism for drumlin formation. Geological Society, London, Special Publications 176 (1), 307–319.
Fowler, A.C., 2018. The philosopher in the kitchen: the role of mathematical modelling in explaining drumlin formation. GFF 140 (2), 93–105.
Francek, M.A., 1991. A spatial perspective on the New York drumlin field. Phys. Geogr. 12, 1–18.
Franzi, D.A., Ridge, J.C., Pair, D.L., Desimone, D., Ratburn, J.A., Barclay, D.J., 2016. Post Valley Heads deglaciation of the Adirondack Mountains and adjacent lowlands. Adirond. J. Environ. Stud. 21, 119–146.
Fullerton, D.S., 1986. Stratigraphy and correlation of glacial deposits from Indiana to New York and New Jersey. In: Sibrava, V., Bowen, D.Q., Richmond, G.M. (Eds.), Quaternary Glaciations of the Northern Hemisphere, vol. 5. Quat. Sci. Rev., pp. 23–37
Glasser, N.F., Jennings, S.J.A., Hambrey, M.J., Hubbard, B., 2015. Origin and dynamic significance of longitudinal structures ("flow stripes") in the Antarctic Ice Sheet. Earth Surf. Dyn. 3, 239–249.
Goldthwait, J.W., 1922. Compiler. Map illustrating recession of the last ice sheet from New England and New York. In: Antevs, E. (Ed.), The Recession of the Last Ice Sheet in New England, vol. 11. American Geographical Research Series, p. 120.
Goldthwait, R.P., Dreimanis, A., Forsyth, J.L., Karrow, P.F., White, G.W., 1965. Pleistocene deposits of the Erie Lobe. In: Wright, H.E., Frey, D.G. (Eds.), The Quaternary of the United States. Princeton University Press, New Jersey, pp. 85–98.
Gravenor, C.P., 1953. The origin of drumlins. Am. J. Sci. 251, 674–681.
Gravenor, C.P., 1957. Surficial geology of the Lindsay-Peterborough area. Geol. Surv. Can. Map 288, 121.
Hart, J.K., 1999. Identifying fast ice flow from landform assemblages in the geological record: a discussion. Ann. Glaciol. 28, 59–66.
Hemming, S.R., 2004. Heinrich Events: massive Late Pleistocene detritus layers of the North Atlantic and its global climate imprint. Rev. Geophys. 42, RG1005.
Hess, D.P., Briner, J.P., 2009. Geospatial analysis of controls on subglacial bedform morphometry in the New York Drumlin Field – implications for Laurentide Ice Sheet dynamics. Earth Surf. Process. Landforms 34, 1126–1135.
Holmes, C.D., 1937. Glacial erosion in a dissected plateau. Am. J. Sci. XXXM, 217–232.
Holmes, C.D., 1952. Drift dispersion in west-central New York. Geol. Soc. Am. Bull. 63, 993–1010.
Holschuh, N., Christianson, K., Paden, J., Alley, R.B., Anandakrishnan, S., 2020. Linking postglacial landscapes to glacier dynamics using swath radar at Thwaites Glacier, Antarctica. Geology 48 (3), 268–272.
Hubbard, G.D., 1906. Drumlinoids of the Catatonk folio. Bull. Am. Geogr. Soc. N. Y. 38, 355–365.
Hughes, T., 1987. Ice dynamics and deglaciation models when ice sheets collapsed. In: Ruddiman, W.F., Wright, H.E. (Eds.), North America and Adjacent Oceans during the Last Deglaciation. Geological Society of America, volume K-3, pp. 183–221.
Isachsen, Y.W., Landing, E., Lauber, J.M., Rickard, L.V., Rogers, W.B., 2000. Geology of New York. A Simplified Account, second ed. New York State Museum, Albany, New York.
Iverson, N.R., McCracken, R.G., Zoet, L.K., Benediktsson, Í.Ö., Schomacker, A., Johnson, M.D., Woodard, J., 2017. A theoretical model of drumlin formation based on observations at Múlajökull, Iceland. J. Geophys. Res. Earth Surf. 122 (12), 2302–2323.
Kappel, W.M., Miller, T.S., 2003. Hydrogeology of the Tully Trough in Southern Onondaga County and Northern Cortland County. U.S. Geological Survey Water-Resources Investigations Report 2003–4112, New York, p. 17.
Karig, D.E., Miller, T.S., 2020. Northward subglacial drainage during the Mackinaw Interstade in the Cayuga basin, central New York, USA. Can. J. Earth Sci. 57 (8), 981–998.
Kerr, M., Eyles, N., 2007. Origin of drumlins on the floor of Lake Ontario and Upper New York State. Sediment. Geol. 193, 7–20.
Krabbendam, M., Eyles, N., Putkinen, N., Bradwell, T., Arbelaez-Moreno, L., 2016. Streamlined 'hard beds' cut by paleo-ice streams: a preliminary review. Sediment. Geol. 338, 24–50.
Krall, D.B., 1977. Late Wisconsinan ice recession in east-central New York. Geol. Soc. Am. Bull. 88, 1697–1710.
Lage, J.P., Assunção, R.M., Reis, E.A., 2001. A minimal spanning tree algorithm applied to spatial cluster analysis. Electron. Notes Discrete Math. 7, 162–165.
Livingstone, S.J., Clark, C.D., 2016. Morphological properties of tunnel valleys of the southern sector of the Laurentide Ice Sheet and implications for their origin. Earth Surf. Dyn. 4, 567–589.
Livingstone, S.J., O'Cofaigh, C.O., Stokes, C.R., Hillenbrand, C.D., Vieli, A., Jamieson, S.S.R., 2012. Antarctic palaeo-ice streams. Earth Sci. Rev. 111, 90–128.
Livingstone, S.J., Stokes, C.R., O Cofaigh, C., Hillenbrand, C.D., Vieli, A., Jamieson, S.S.R., Spagnolo, M., Dowdeswell, J., 2016. Subglacial processes on an Antarctic ice stream bed. 1. Sediment transport and bedform genesis inferred from marine geophysical data. J. Glaciol. 62, 270–284.
Margold, M., Stokes, C.R., Clark, C.D., Kleman, J., 2015a. Ice streams in the Laurentide Ice Sheet: a new mapping inventory. J. Maps 11, 380–395.
Margold, M., Stokes, C.R., Clark, C.D., 2015b. Ice streams in the Laurentide Ice Sheet: Identification, characteristics and comparison to modern ice sheets. Earth Sci. Rev. 143, 117–146.
Margold, M., Stokes, C.R., Clark, C.D., 2018. Reconciling records of ice streaming and ice margin retreat to produce a paleogeographic reconstruction of the deglaciation of the Laurentide Ice Sheet. Quat. Sci. Rev. 189, 1–30.
McClenaghan, M.B., Paulen, R.C., 2017. Mineral Exploration in Glaciated Terrain. In: Menzies, J., Van Der Meer, J.J.-M. (Eds.), Past Glacial Environments, second ed. Elsevier, Amsterdam, pp. 689–751.
McClenaghan, M.B., Paulen, R., Kjarsgaard, I.M., 2018. Rare metal indicator minerals in bedrock and till at the Strange Lake peralkaline complex, Quebec and Labrador. Can. J. Earth Sci. 56, 857–869.
Millar, S.W., 2004. Identification of mapped ice margin positions in western New York State from digital terrain-analysis and soil databases. Phys. Geogr. 25, 347–359.
Miller, J.W., 1972. Variations in New York drumlins. Ann. Assoc. Am. Geogr. 62, 418–423.
Miller, J.W., 1974. A discontinuous surface on the Central New York drumlin field. Trans. N. Y. Acad. Sci. 36, 391–395.
Monnett, V.E., 1924. The Finger Lakes of central New York. Am. J. Sci. 8, 33–53.
Muller, E.H., 1965a. Quaternary geology of New York. In: Wright, H.E., Frey, D.G. (Eds.), The Quaternary of the United States. Princeton University Press, pp. 99–112.
Muller, E.H., 1965b. Bibliography of New York Quaternary Geology. N. Y. State Mus. Bull. 398, 116.

Muller, E.H., Cadwell, D.H., 1986. Surficial geologic map of the New York Finger Lakes Sheet. New York State Museum. Albany, Geological Survey Map and Chart Series #40, 1:250,000.
Muller, E.H., Calkin, P.E., 1993. Timing of Pleistocene glacial events in New York State. Can. J. Earth Sci. 30, 1829–1845.
Muller, E.H., Prest, V.K., 1985. Glacial lakes in the Ontario Basin. In: Karrow, P.F., Calkin, P.E. (Eds.), Quaternary Evolution of the Great Lakes. Geological Association of Canada, Special Paper 30, pp. 213–229.
Muller, E.H., Braun, D.D., Young, R.A., Wilson, M.P., 1988. Morphogenesis of the Genesee Valley. Northeast. Geol. 10, 112–133.
Subsurface Geologic Investigations of New York Finger Lakes: Implications for late Quaternary Deglaciation and Environmental Change. In: Mullins, H.T., Eyles, N. (Eds.), Geol. Soc. Am. Spec. Pap. 311.
Mullins, H.T., Hinchey, E.J., 1989. Erosion and infill of New York Finger Lakes: Implications for Laurentide ice sheet deglaciation. Geology 17 (7), 622–625.
Mullins, H.T., Eyles, N., Hinchey, E.J., 1991. High resolution seismic stratigraphy of Lake McDonald, Glacier National Park, Montana, U.S. A. Arct. Alp. Res. 23, 311–319.
Mullins, H.T., Hinchey, E.J., Wellner, R.W., Stephens, D.B., Anderson, W.T., Dwyer, T.R., Hine, A.C., 1996. Seismic stratigraphy of the Finger Lakes: A continental record of Heinrich Event H-1 and Laurentide Ice Sheet instability. In: Mullins, H.T., Eyles, N. (Eds.), Subsurface Geologic Investigations of New York Finger Lakes: Implications for Late Quaternary Deglaciation and Environmental Change. Geological Society of America. Special Paper 311, pp. 1–36.
Ng, F.S.L., Hughes, A.L.C., 2019. Reconstructing ice-flow fields from streamlined subglacial bedforms: A kriging approach. Earth Surf. Process. Landforms 44, 861–876.
Occhietti, S., Parent, M., Shilts, W.W., Dionne, J.C., Govare, E., Harmand, D., 2001. Late Wisconsinan glacial dynamics, deglaciation, and marine invasion in southern Quebec. In: Weddle, T.K., Retelle, M.J. (Eds.), Deglacial History and Relative Sea-Level Changes, Northern New England and Adjacent Canada. Geological Society of America. Special Paper 351, Boulder, Colorado, pp. 243–270.
Ó Cofaigh, C., Evans, D.J.A., Smith, I.R., 2010. Large-scale reorganization and sedimentation of terrestrial ice streams during late Wisconsinan Laurentide Ice Sheet deglaciation. Geol. Soc. Am. Bull. 122, 743–756.
Ó Cofaigh, C., Stokes, C.R., Lian, O.B., Clark, C.D., Tulaczyk, S., 2013. Formation of mega-scale glacial lineations on the Dubawnt Lake Ice Stream bed: 2. Sedimentology and stratigraphy. Quat. Sci. Rev. 77, 210–227.
Otteson, D., Stokes, C.R., Bøe, R., Rise, L., Longva, O., Thorsnes, T., Olesen, O., Bugge, T., Lepland, A., Hestvik, O.B., 2016. Landform assemblages and sedimentary processes along the Norwegian Channel Ice Stream. Sediment. Geol. 338, 115–137.
Paulen, R.C., McClenaghan, M.B., Harris, J., 2006. Bedrock topography and drift thickness models from the Timmins area, northeastern Ontario: an application of GIS to the Timmins overburden drillhole database. In: Harris, J., Wright, D., Berdusco, B. (Eds.), GIS Applications in the Earth Sciences, vol. 44. Geological Association of Canada, Special Publication, pp. 413–434.
Paulen, R.C., Stokes, C.R., Fortin, R., Rice, J.M., Dube-Loubert, H., McClenaghan, M., 2017. Dispersal trains produced by ice streams: an example from Strange Lake, Labrador, Canada. In: Tschirhart, V., Thomas, M.D. (Eds.), Proceedings of Exploration 17. Sixth Decennial International Conference on Mineral Exploration, pp. 871–875.
Putkinen, N., Eyles, N., Putkinen, S., Ojala, A.E., Palmu, J.P., Sarala, P., Väänänen, T., Räisänen, J., Saarelainen, J., Ahtonen, N., Rönty, H., 2017. High-resolution LiDAR mapping of glacial landforms and ice stream lobes in Finland. Bull. Geol. Soc. Finland 89 (2).
Rasmussen, S.O., Andersen, K.K., Svensson, A.M., Steffensen, J.P., Vinther, B.M., Clausen, H.B., Siggaard-Andersen, M.L., Johnsen, S.J., Larsen, L.B., Dahl-Jensen, D., Bigler, M., Röthlisberger, R., Fischer, H., Goto-Azuma, K., Hansson, M.E., Ruth, U., 2006. A new Greenland ice core chronology for the Last Glacial Termination. J. Geophys. Res. 111, D06102.
Rayburn, J.A., Knuepfer, P.L.K., Franzi, D.A., 2005. A series of large, Late Wisconsinan meltwater floods through the Champlain and Hudson Valleys, New York State, USA. Quat. Sci. Rev. 24, 2410–2419.
Ridge, J.C., 2003. The last deglaciation of the Northeastern United States: a combined varve, paleomagnetic, and calibrated 14C chronology. In: Cremeens, D.L., Hart, J.P. (Eds.), Geoarchaeology of Landscapes in the Glaciated Northeast, vol. 497. New York State Museum Bulletin, pp. 15–48.
Ridge, J.C., 2004. The Quaternary glaciation of western New England with correlations to surrounding areas. In: Ehlers, J., Gibbard, P.L. (Eds.), Quaternary Glaciations –Extent and Chronology, Part II: North America. Developments in Quaternary Science 2B. Elsevier, Amsterdam, pp. 163–193.
Ridge, J., Franzi, D.A., Muller, E.H., 1991. Late Wisconsinan, pre-Valley Heads glaciation in the western Mohawk Valley, central New York, and its regional implications. Bull. Geol. Soc. Am. 103, 1032–1048.
Ridge, J.C., Balco, G., Bayless, R.L., Beck, C.C., Carter, L.B., Dean, J.L., Voytek, E.B., Wei, J.H., 2012. The new North American varve chronology: A precise record of southeastern Laurentide Ice Sheet deglaciation and climate, 18.2-12.5 kyr BP, and correlations with Greenland ice core records. Am. J. Sci. 312, 685–722.
Ridky, R.W., Bindschadler, R.A., 1990. Reconstruction and dynamics of the late Wisconsin Ontario ice dome in the Finger Lakes region, New York. Geol. Soc. Am. Bull. 102, 1055-1064.
Rose, J., 1987. Drumlins as part of glacier bedform continuum. In: Drumlin Symposium, pp. 103–116.
Ross, M., Parent, M., Benjumea, B., Hunter, J., 2006. The late Quaternary stratigraphic record northwest of Montréal: regional ice-sheet dynamics, ice-stream activity, and early deglacial events. Can. J. Earth Sci. 43, 461–485.
Ross, M., Campbell, J.E., Parent, M., Adams, R.S., 2009. Paleo-ice streams and the subglacial landscape mosaic of the North American mid-continental prairies. Boreas 38, 421–439.
Shepps, V.C., White, G.W., Droste, J.B., Sitler, R.F., 1959. Glacial geology of northwestern Pennsylvania. Pennsylvania Geological Survey, 4th series, Gen. Geol. Rep. 32, 59.
Sibson, R., 1981. A brief description of natural neighbour interpolation. In: Barnett, V. (Ed.), Interpreting Multivariate Data. Wiley, London, pp. 21–26.
Slater, G., 1929. The structure of the drumlins exposed on the south shore of Lake Ontario. N. Y. State Mus. Bull. 281, 3–19.
Smalley, I.J., Unwin, D.J., 1968. The formation and shape of drumlins and their distribution and orientation in drumlin fields. J. Glaciol. 7 (51), 377–390.
Smith, A.M., Bentley, C.R., Bingham, R.G., Jordan, T.A., 2012. Rapid subglacial erosion beneath Pine Island Glacier, West Antarctica. Geophys. Res. Lett. 39, L12501.
Sookhan, S., Eyles, N., Putkinen, N., 2016. LiDAR-based volume assessment of the origin of the Wadena Drumlin Field. Minnesota, USA. Sediment. Geol. 338, 72–83.
Sookhan, S., Eyles, N., Putkinen, N., 2018a. LiDAR-based mapping of paleo-ice streams in the eastern Great Lakes sector of the Laurentide Ice Sheet and a model for the evolution of drumlins and megascale glacial lineations. J. Geol. Soc. Swed. 140, 202–228.
Sookhan, S., Eyles, N., Arbelaez-Moreno, L., 2018b. Converging ice streams: a new paradigm for reconstruction of the Laurentide Ice Sheet in southern Ontario and deposition of the Oak Ridges Moraine. Can. J. Earth Sci. 55, 373–396.
Sookhan, S., Eyles, N., Arbelaez-Moreno, L., 2019. Converging ice streams: a new paradigm for reconstruction of the Laurentide Ice Sheet in southern Ontario and deposition of the Oak Ridges Moraine. Reply to Comments: Can. J. Earth Sci. 56 (8), 889–893.
Spagnolo, M., Clark, C.D., Hughes, A.L., 2012. Drumlin relief. Geomorphology 153, 179–191.
Spagnolo, M., Clark, C.D., Ely, J.C., Stokes, C.R., Anderson, J.B., Andreassen, K., Graham, A.G., King, E.C., 2014. Size, shape and spatial arrangement of mega-scale glacial lineations from a large and diverse dataset. Earth Surf. Process. Landforms 39, 1432–1448.
Stanford, J.D., Rohling, E.J., Bacon, S., Roberts, A.P., Grousset, F.E., Bolshaw, M., 2011. A new concept for the paleo-oceanographic evolution of Heinrich event 1 in the North Atlantic. Quat. Sci. Rev. 30, 1047–1066.
Stokes, C.R., Clark, C.D., 2002. Are long subglacial bedforms indicative of fast ice flow? Boreas 31 (3), 239–249.
Stokes, C.R., Clark, C.D., 2003. The Dubawnt Lake palaeo-ice stream: evidence for dynamic ice sheet behaviour on the Canadian Shield and insights regarding the controls on ice-stream location and vigour. Boreas 32 (1), 263–279.
Stokes, C.R., 2011. Paleo-Ice Stream. In: Bishop, M.P., Björnsson, H., Haeberli, W., Oerlemans, J., Shroder, J.F., Tranter, M. (Eds.), Encyclopedia of Snow, Ice and Glaciers. Springer Science & Business Media, Dordrecht, Netherlands, pp. 127–128.
Stokes, C.R., Fowler, A.C., Clark, C.D., Hindmarsh, R.C., Spagnolo, M., 2013. The instability theory of drumlin formation and its explanation of their varied composition and internal structure. Quat. Sci. Rev. 62, 77–96.
Stokes, C.R., Margold, M., Clark, C.D., Tarasov, L., 2016. Ice stream activity scaled to ice sheet volume during Laurentide Ice Sheet deglaciation. Nat 530, 322–326.
Tarr, R.S., 1894. Cayuga Lake. A rock basin. Geol. Soc. Am. Bull. 5, 339–356.
Tarr, R.S., 1905. Drainage features of Central New York. Geol. Soc. Am. Bull. XVI, 229–242.
Taylor, F.B., 1913. Moraine systems of Southwestern Ontario. R. Can. Inst. Trans. 10, 57–79.
Thomas, R.H., 1977. Calving bay dynamics and ice sheet retreat up the St. Lawrence valley system. Géogr. phys. Quat. XXXI, 347–356.
Van Fossen, F., Kent, D.V., 1993. A Palaeomagnetic study of 143 Ma kimberlite dikes in central New York State. Geophys. J. Int. 113, 175–185.
Virden, W., Warren, J., Holcombe, D., Reid, D., Berggren, T., 1999. Bathymetry of Lake Ontario. National Oceanic and Atmospheric Administration, CD-Rom, G2.
Wellner, R.W., Petruccione, J.L., Sheridan, R.E., 1996. Correlation of drill core and geophysical results from Canandaigua Lake Valley, New York: Evidence for rapid late-glacial sediment infill. In: Mullins, H.T., Eyles, N. (Eds.), Subsurface Geologic Investigations of the New York Finger Lakes: Implications for Late Quaternary Deglaciation and Environmental Change. Geological Society of America. Special Paper 311, pp. 37–49.
White, W.A., 1985. Drumlins carved by rapid water-rich surges. Northeast. Geol. 7, 161-166.
Winsborrow, M.C.M., Stokes, C.R., Andreassen, K., 2012. Ice stream flow switching during deglaciation of the southwestern Barents Sea. Geol. Soc. Am. Bull. 124, 275–290.
Yu, P., Eyles, N., Sookhan, S., 2015. Automated drumlin shape and volume estimation using high resolution LiDAR imagery (Curvature Based Relief Separation): A test from the Wadena Drumlin Field, Minnesota. Geomorphology 246, 589–601.
Zaremba, N.J., Scholz, C.A., 2019. High-resolution seismic stratigraphy of Late Pleistocene Glacial Lake Iroquois and its Holocene successor: Oneida Lake. New York Palaeogeogr. Palaeoclimatol. Palaeoecol. 534, 109286.